ADDIS ABABA UNIVERSITY

ADDIS ABABA INSTITUTE OF TECHNOLOGY

SCHOOL OF CIVIL AND ENVIRONMENTAL ENGINEERING

The Effect of Longitudinal Reinforcement End Anchorage Angle and Development Length from the support in Beam Capacity

A Thesis in Structural Engineering

By Abiy Ayenew

October 4, 2019

Addis Ababa

A Thesis

Submitted in Partial Fulfillment of the Requirements for the Degree of Master of Science

The undersigned have examined the thesis entitled '**The Effect of Longitudinal Reinforcement End Anchorage Angle and Development Length from the support in Beam Capacity'** presented by **Abiy Ayenew**, a candidate for the degree of **Master of Science** and hereby certify that it is worthy of acceptance.

Advisor	Signature	Date
Internal Examiner	Signature	Date
External Examiner	Signature	Date
Chairperson	Signature	Date

UNDERTAKING

I certify that research work titled "The Effect of Longitudinal Reinforcement End Anchorage Angle and Development Length from the support in Beam Capacity" is my own work. The work has not been presented elsewhere for assessment. Where material has been used from other sources it has been properly acknowledged/referred.

Abiy Ayenew

ABSTRACT

In reinforced concrete members, reinforcement must be bonded or anchored to the concrete. Reinforcement development length is provided in the regions of maximum stress to zero stress. However, at the support of simply supported beam, the bending stress is zero, the researchers recommend that the longitudinal reinforcement should develop farther from the support to resist pullout of bars. The research focuses on the investigation of the effect of longitudinal reinforcement end anchorage angle and development length from the support on simply supported beam capacity. The investigation was conducted on three shear critical and three flexure critical beams using experiment and finite element analysis software. The experimental and the finite element analysis result gives comparable result for each beam. The result shows that the development of a longitudinal reinforcement bar farther from the center of support and use of 135^o or 90^o end anchorage angle has no significant effect on flexure critical beams capacity and crack pattern formation. But, use of development length and different end anchorage angles on longitudinal reinforcement bars have a significant effect on the ultimate load capacity and crack pattern formation on the shear critical beams. The ultimate capacities of beams having longitudinal reinforcement 135^o end anchorage and beams without development length from the support reduced by 11.75% and 29.05% from the ultimate capacities of beams having 90^o end anchorage respectively. Also, shear critical beams give different crack pattern formation due to the variation of reinforcement bar end anchorage angle and development length.

ACKNOWLEDGMENTS

I would like to express my sincere appreciation to Dr. Adil Zekaria for his guidance in completing the research work. His advice and encouragement during the preparation of this report are sincerely appreciated.

My deepest thanks go to all the Civil and Environmental Engineering Department of Addis Ababa University instructors for their guidance and support to this research and the non-teaching staff.

I am also thankful to all AAiT Construction Material Laboratory staff members for their cooperation and help during the experimental program and to my family their financial support and inspiration from the beginning to the end of the work.

TABLE OF CONTENTS

LIST OF TABLES

LIST OF FIGURES

CHAPTER 1 INTRODUCTION

1.1 General Background

Beams are structural elements carrying external loads that cause bending moments, shear forces and torsional moments along the section length. The structural details of such beams must resist bending, diagonal tension, shear, and torsion and must be such as to transmit forces a bond without causing internal cracking. In reinforced concrete members, reinforcement must be bonded or anchored to the concrete so that it can develop its yield strength at sections subjected to maximum stresses. This is often accomplished by embedding the reinforcement far enough on either side of the critical section so that it is anchored by a combination of mechanical interlock and friction with the surrounding concrete. The reinforcement in an RC structure, such as a steel bar, has nothing to do with the anchorage the same strain or deformation as the surrounding concrete in order to prevent discontinuity, slip or separation of the two materials under load. Maintaining composite action requires the transfer of load between the concrete and steel. The direct stress is transferred from the concrete to the bar interface so as to change the tensile stress in the reinforcing bar along its length. This load transfer is achieved by means of bond (anchorage) and is idealized as a continuous stress field that develops in the vicinity of the steel-concrete interface. In many cases, however, such as exterior beam-column joints, the concrete dimensions are not adequate to fully develop the yield strength of the bar. In these cases, anchorage is often obtained through the use of hooked bars. In simply supported reinforced concrete beams the common type of reinforcement end anchorage recommends in most civil engineering codes (ACI) is a right angle or 90^{o}.

1.2 Significance

The research will have huge significance in the economical construction of reinforced concrete members. It may increase the flexural and shear resistance capacity of the reinforced concrete beam through identifying the effective reinforcement end anchorage angle which maximizes the bond between reinforcement bar and plain concrete.

1.3 Statement of the Problem

A development length or anchorage can be defined as the amount of reinforcement bar length needed to be embedded or projected into the member to establish the desired bond strength between the concrete and steel. The aim of providing development length is to develop a safe bond between the bar surface & the concrete so that no failure due to slippage of bar occurs during the ultimate load conditions. ACI Code expresses development length as the shortest length of a bar in which the bar stress can increase from zero to the yield strength. When we see simply supported beams, the bending moment is zero at the support. The development of longitudinal reinforcement needed is from the mid-span to the center of the support since the bending moment at the support in simply supported beam is zero. But Azlina et al studies and confirm that a significant amount of tensile force exists in the support region due to the occurrence of the diagonal shear cracks. He suggests that longitudinal reinforcement in the shear span zone must be sufficiently extended into the support to avoid bond-splitting failure due to some shifting of the tensile force. Also, Mylrea (1948) suggested that extending the bar past the support may result in a better tensile force distribution and provide higher bond capacity. In the above discussions, there are two ideas about the development of longitudinal reinforcement from the support. In the other case, developing or anchoring of longitudinal reinforcement bars further from the support with 135^{o} (parallel to shear crack patterns) may reduce the shear capacities of shear critical beams. This case needs research to decide which idea is more suitable to get maximum beam capacity both in flexure critical and shear critical beams.

1.4 Objectives

1.4.1 General Objective

To investigate the effect of longitudinal reinforcement end anchorage angle and development length from the support on the flexure and shear capacities of simply supported beams.

1.4.2 Specific Objective

- To assess the effect of longitudinal reinforcement end anchorage angle and development length from the support on the ultimate shear and flexural capacity of simply supported beams.

- To visualize the crack formations on shear critical and flexure critical beams due to the variation of longitudinal reinforcement end anchorage angle and development length from the center of the support.

- To visualize the effect of longitudinal reinforcement end anchorage angle and development length on the load vs deflection diagram of simply supported beams.

1.5 Scope

The work was conducted only on simply supported beams. The effect of shear reinforcement anchorage is not considered in this work. For the whole beam specimens, the same shear reinforcement anchorage was used.

The beam specimens were flexure critical and shear critical simply supported beams with the following characteristics:

- Beam specimen's longitudinal reinforcement with development length and 90^o end anchorage angle.
- Beam specimen's longitudinal reinforcement with development length and 135^o end anchorage angle.
- Beam specimen's longitudinal reinforcement without development length from the support.

In the investigation of the research, only beam's shear and flexural resistance capacities, crack patterns and load vs deflection diagrams were considered. Torsional, service load, long-term loading, the effect of creep, shrinkage and other parameters were not covered.

1.6 Methodology

The overall process of this research includes literature review, experimental program and analytical simulation using non-linear finite element analysis VecTor2 software modeling.

First, the experimental investigation was conducted in Addis Ababa University in the AAiT construction material laboratory. In this investigation, the material characterization tests of cement, fine aggregate (sand), coarse aggregate were determined. After the determination of material characterization result the mix design was prepared and the fresh and mechanical properties of plain concrete and the mechanical properties of steel reinforcement were determined.

A total of six beam specimens, three of them shear critical and the rest are flexure critical beams were cast according to different bar anchorage arrangements from the support. As the beams getting their full strength or after 28 days from casting the beams were tested in AAiT construction material laboratory.

Like that of the experimental investigation, the beams were modeled in VecTor2 finite element software to compare with the experimental result.

The results found in the experimental result and in the finite element software were compared to each other and also the effect of longitudinal reinforcement end anchorage angle on shear and flexure beam capacity was determined and the discussion was made.

1.7 Layout of Chapters

The first chapter discusses the general about anchorage and development length of the reinforcement bar. The statement of the problem, objective of the thesis, significance, and methodologies of how the research was conducted throughout the research work was presented.

The second chapter discusses the past works on the bond between reinforcement bar and concrete, development length & anchorage of longitudinal reinforcement, shear failure mechanism, and anchorage, longitudinal tensile reinforcement contribution to shear strength and reinforcement detailing of simply supported beams.

The third chapter focuses on the experimental program carried out to cast the concrete beam specimens. Material characterization test results of constituent materials and the resulting concrete and reinforcement material property test procedures are presented. The procedures and methods used in the specimen preparation including mix design, casting, and curing and test setup preparation are also included.

The fourth chapter discusses the modeling of beam specimens on VecTor2 software to compare with the experimental investigation. It presents the procedures taken to model specimens including models used for concrete materials, material properties, and specimen detailing.

The fifth chapter mainly focuses on the test results found from the experiment and finite element analysis. In this chapter, a detailed analysis of crack patterns and load vs deflection diagrams of each flexure and shear critical beams were discussed.

The sixth chapter summarizes the main findings found from the thesis and also provides additional information on further works and recommendations. In the last part references and appendix are included.

CHAPTER 2 LITERATURE REVIEW

2.1 Introduction

In this chapter, a brief review of the literature on anchorage and development length effect in simply supported beams was discussed. The bond between reinforcement bar and concrete, development length & anchorage of longitudinal reinforcement, shear failure mechanism and anchorage, longitudinal tensile reinforcement contribution to shear strength and reinforcement detailing of simply supported beams of the past works were included.

2.2 Bond Strength between Reinforcement Bar and Concrete

One of the fundamental assumptions of reinforced concrete design is that at the interface of the concrete and the steel bars exists perfect bonding and no slippage occurs. Based on these assumptions, it follows that some form of bond stress exists at the contact surface between the concrete and the steel bar.

Mashhour and Mahmoud El-Mihilmy (2008) suggested that bond strength results from several factors, such as the adhesion between the concrete and steel interfaces and the pressure of the hardened concrete against the steel bar. In a reinforced concrete beam, the flexural compressive forces are resisted by concrete, while the flexural tensile forces are provided by reinforcement as shown in Figure 2-1. For this process to exist, there must be a force transfer or bond between the two materials.

The force acting on the bar shown in Figure 2-1, to be in equilibrium, bond stress, f_b, must exist. If this disappears, the bar will pull out of the concrete and the tensile force, T, will drop to zero, causing the beam to fail.

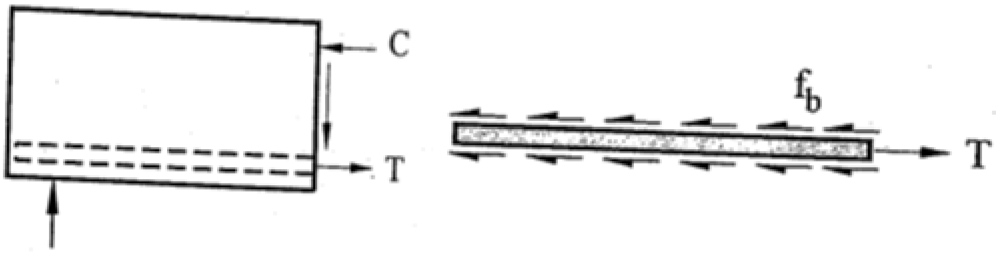

Figure 2-1: Force acting on a bar (source design reinforced concrete structure book)

James G. Macgregor (2009) in his book, at the cracks in a beam, the bar force is high. If the concrete and the bar are bonded together, a portion of the tensile force will be resisted by the concrete at points between the cracks. As a result, the tensile stresses in steel and the concrete at the level of the steel will vary.

2.3 Development Length & Anchorage of Longitudinal Reinforcement

Many researchers and books agreed that longitudinal reinforcement bars of simply supported beam need anchorage or bond at the end of the beam. Reinforcing bars, wires or welded mesh fabrics shall be so anchored that the bond forces are safely transmitted to the concrete avoiding longitudinal cracking. The ultimate bond strength shall be sufficient to prevent bond failure. ACI 318-08 requires that the reinforcement shall extend into the support (La) at least 150 mm to provide end anchorage see Figure 2-2. Alternatively, the end hook shape can be used as anchorage. This method is the most commonly used in reinforced concrete structures with steel bars.

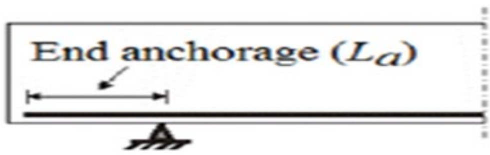

Figure 2-2: Anchorage of bars beyond the support

The ACI Code now contains development length provisions for the use of headed or mechanically anchored deformed reinforcing bars in tension. The development length for a headed bar generally will be shorter than that for a hooked bar, so it may be advantageous to use headed bars where there is limited space available to develop bars in tension.

Rendy Thamrin (2016) decide that end anchorage beyond the support has an important role in improving the bond capacity of the beams. The beams with insufficient length of end anchorage failed in bond-splitting failure mode due to premature bond loss at the support zone indicated by the occurrence of bond splitting cracks developing toward the support, while beams with sufficient end anchorage length failed in flexure or shear mode depending on the number of stirrups. Rendy Thamrin (2016) predicted bond stress distributions along the concrete rectangular prism using numerical procedure shows a uniform distribution of bond stresses along insufficient end anchorage with very high values. Meanwhile more reasonable profiles of bond stress distributions along end anchorage are shown in case of adequate end anchorage length.

Mylrea (1948) suggested that extending the bar past the support may result in a better tensile force distribution and provide higher bond capacity. Pay et al. (2014) recently reports that flexural bond strength is affected by modulus elasticity and axial rigidity of longitudinal reinforcement. It is also confirmed in their report that the bond length in the splice region affects bond strength. The test result clarified by Pay et al. supports the previous report described by concerning the requirement of bond length of tensile reinforcement. Azlina et al studies and confirm that a significant amount of tensile force exists in the support region due to the occurrence of the diagonal shear cracks. He suggests that longitudinal reinforcement in the shear span zone must be sufficiently extended into the support to avoid bond-splitting failure due to some shifting of the tensile force.

James G. Macgregor (2009) the development length is the shortest length of bar in which the bar stress can increase from zero to the yield strength, If the distance from a point where the bar stress equals to the end of the bar is less than the development length, the bar will pull out of the concrete. The development lengths are different in tension and compression because a bar loaded in tension is subject to in-and-out bond stresses and hence requires a considerably longer development length. Also, for a bar in compression, bearing stresses at the end of the bar will transfer part of the compression force into the concrete.

If the flexural reinforcement provided exceeds the amount required to resist the factored moment, the bar stress that must be developed is less than. In such a case, ACI Code

Section 12.2.5 allows to be multiplied by (provided). If room is available, the author recommends ignoring this factor, thus ensuring that the steel is fully anchored. In statically indeterminate structures, the increased stiffness resulting from the additional reinforcement can lead to higher moments at the section with excess reinforcement. In such a case, the steel is more highly stressed than would be expected from the ratio of areas. The development length, calculated as the product of from ACI Code Section 12.2.2 or Section 12.2.3.

Clearly, the detailing of the reinforced concrete members is the key to good design and execution of work at the site. That is why poor detailing of reinforcement makes the structure undergo cracking, excessive deflection, or even collapse. Reinforcements resist tensile forces. Finally, different aspects of reinforced concrete beam detailing based on ACI Code are explained in the following sections.

The function of hooked anchors is the provision of additional anchorage when there is inadequate straight length available to develop a bar. Commonly, standard hooks described in ACI Code Section 7.1 utilized apart from the case where it is specifically specified.

ACI standard hooks for primary reinforcement:

- 180° bend plus 4db extension, but not less than 65mm at free end of bar.
- 90° bend plus 12db extension at the free end of the bar.

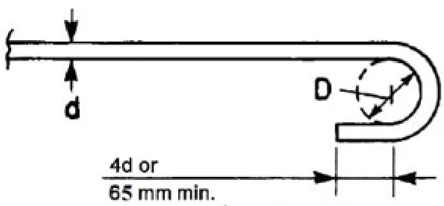

Figure 2-3: Standard hook, 180degree (ACI)

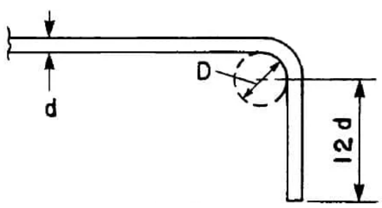

Figure 2-4: Standard hook, 90degree (ACI)

The development length (ld) is the shortest length of the bar in which the bar stress can increase from zero to the yield strength (fy). It is different in tension and compression, and the basic equation for each case are as follow:

ACI recommends development length in tension the following expression, but no less than 30.48cm.

$$l_d = \left\{ \frac{f_y \Psi_t \Psi_e \Psi_s}{1.1\lambda\sqrt{f'_c}\left(\frac{C_b+K_{tr}}{d_b}\right)} \right\} d_b) \qquad \textbf{(2-1)}$$

$$K_{tr} = \frac{40A_{tr}}{sn} \qquad \textbf{(2-2)}$$

Where:

C_b = Factor that represents the smallest of the side cover. The cover over the bar or wire (in both cases measured to the center of the bar or wire)

K_{tr} = Factor which denotes the contribution of confining reinforcement across potential splitting planes.

Ψ_t = The traditional reinforcement location factor to reflect the adverse effects of the top reinforcement casting position.

Ψ_e = Coating factor reflecting the effects of epoxy coating. The product should not exceed 1.7.

Ψ_s= Reinforcement size factor that reflects the more favorable performance of smaller diameter reinforcement.

λ = Factor reflecting the lower tensile strength of lightweight concrete and the resulting reduction of the splitting resistance, which increases the development length in lightweight concrete.

$(C_b + K_{tr})/d_b$ equal to 2.5 if the result of $(C_b + K_{tr})/d_b$ is less than 2.5

d_b = Bar diameter

A_{tr} = Total cross-sectional area of all transverse reinforcement within the spacing S.

n = Number of bars or wires being developed along the plane of splitting

f'_c = Concrete compressive strength

f_y = reinforcment bar yield strength

Development length in compression can be calculated using the greatest of the following formula, but it shall not be smaller than 20.32cm.

$$l_{dc} = (0.02 fy \ / \ ) db \quad \textbf{2-3}$$

$$l_{dc} = ((0.0003 fy) db \quad \textbf{2-4}$$

Where

ldc: development length in compression bars

fy: yield strength of bars

db: bar diameter

2.4 Shear in Beams

2.4.1 Shear Failure Mechanism and Anchorage

Shear failures of beams are characterized by the occurrence of inclined cracks. In some cases, inclined crack is immediately followed by member failure and in other cases, the inclined cracks stabilize and substantially more shear force may be applied before the member fails.

Inclined cracks in the web of a beam may develop either before a flexural crack occurs in their vicinity or as an extension of a previously developed flexural crack. The first type of inclined crack is often referred to as a “web-shear crack”. The second type is often identified as a “flexural-shear crack;” and the flexural crack causing the inclined crack is referred to as the “initiating flexural crack”. in addition to the primary cracks (flexural and the two types of inclined cracks), secondary cracks often result from splitting forces developed by the deformed bars when slip between concrete and steel reinforcement occurs, or from dowel action forces in the longitudinal bars transferring shear across the crack.

Figure 2-5 below shows shear failure crack occurred due to anchorage failure of longitudinal tensile reinforcement as indicated by failure type 1. The anchorage failure occurs due to loss of bond between the concrete and reinforcement steel bar due to splitting cracks. Beam failure modes based on the shear span to depth ratio (a/d) are shown in Figure 2-5.

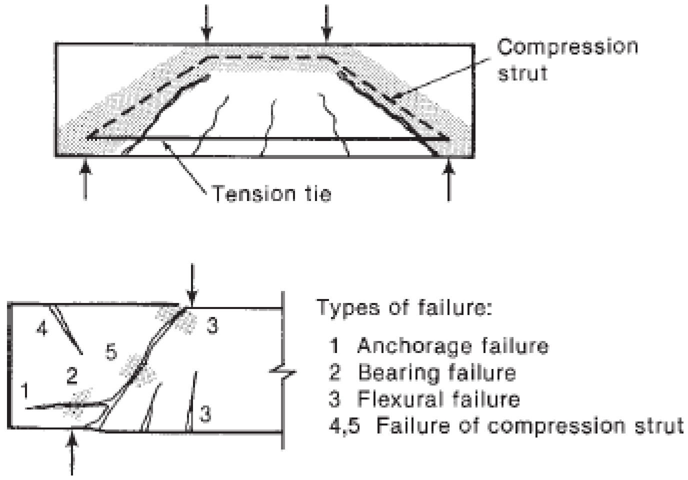

Figure 2-5: Failure mode of deep beams, a/d = 0.5 to 2.0 (Adapted from McGregor)

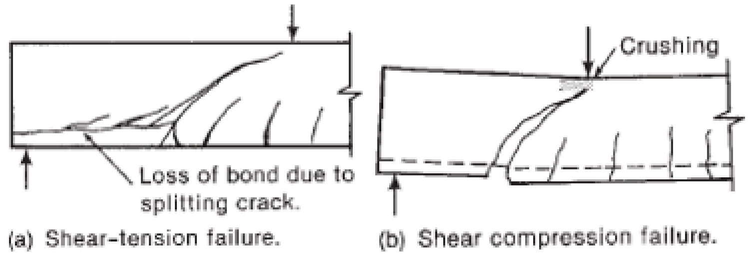

Figure 2-6: Modes of failure, a/d=1.5 to 2.5 [Adapted from MCGregor]

2.4.2 Longitudinal Tensile Reinforcement Contribution to Shear Strength

Mainly the longitudinal tensile reinforcement bars designed for flexural strength of beams. And, stirrups reinforcements designed for shear strength of beams. But researchers suggest that longitudinal tensile reinforcements have a little bit of contribution in the shear strength of beams.

Chang E. H. (2009) conducted an experimental investigation on the longitudinal tensile reinforcement ratio on the shear capacity for beams with the same shear reinforcement ratios. The result shows the shear capacity of the beams increased with the increase of the longitudinal reinforcement ratio.

Tureyen, Ahmet Koray (2001) studied the influence of longitudinal reinforcement on the shear strength of beams. Based on the experimental evidence from steel-reinforced concrete shear tests, he concludes that the use of low longitudinal reinforcement ratios can cause a reduction in shear strength.

The contribution of longitudinal reinforcement on shear strength of reinforced concrete beam may be affected by arrangement and anchorage angle of longitudinal reinforcement.

2.5 Simply Supported beams Reinforcement Detailing Overview

For a long period of time, researchers conducted research on structural members for different purposes. The reinforced concrete beam is one of a structural member. Many researchers conducted on beams to investigate the behavior of beam on flexural strength, shear strength, torsional strength, etc. M.Y.H. Bangash (1992) provides reinforcement detailing of simply supported beam, on his book, to carry external loads that cause bending moments, shear forces as shown in Figure 2-7. It shows that both the tensile and compression reinforcement were anchored or developed from the support.

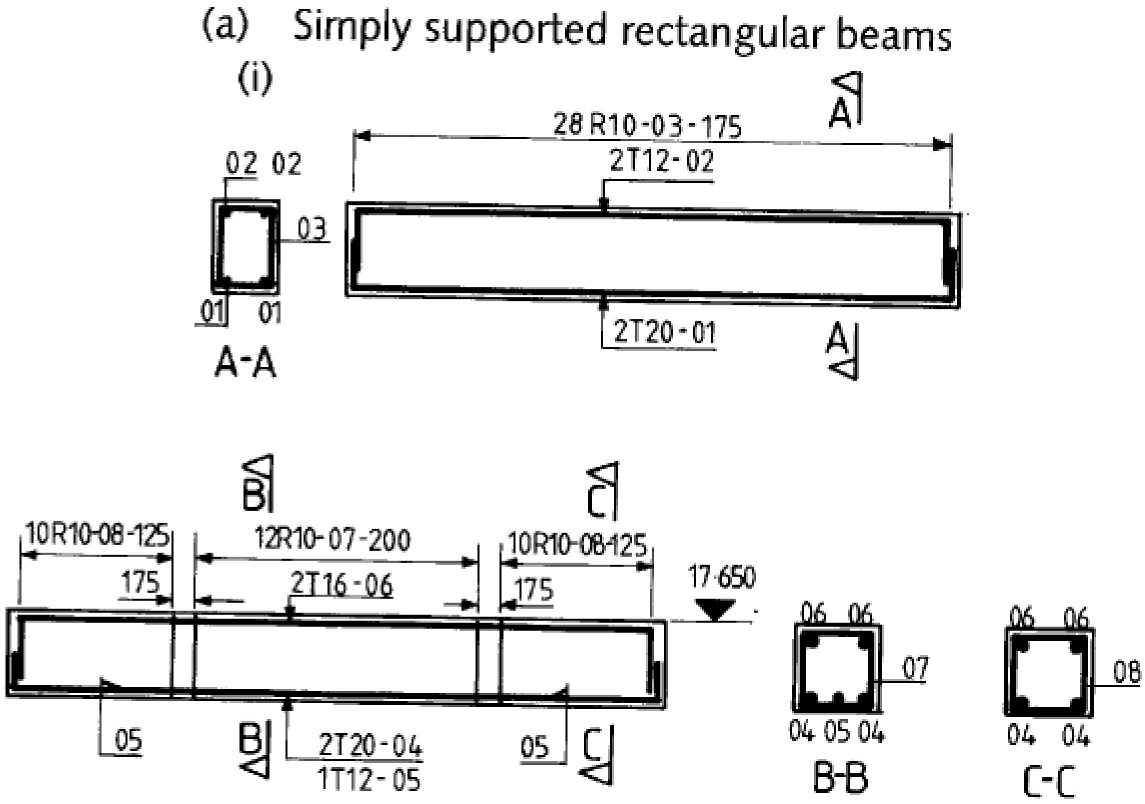

Figure 2-7: Simply supported beam detailing

Rami A. et al (2014) conducted a research on the behavior of reinforced concrete beams strengthened with externally bonded hybrid fiber-reinforced polymer systems. The research was focused on the flexural strength of beams with different fibber reinforced polymer materials. The arrangement and detailing of reinforcement bars for the research sample beam was shown in Figure 2-8. In this figure, the longitudinal reinforcement bar was anchored or provided a development length further from the support with 90^{o}.

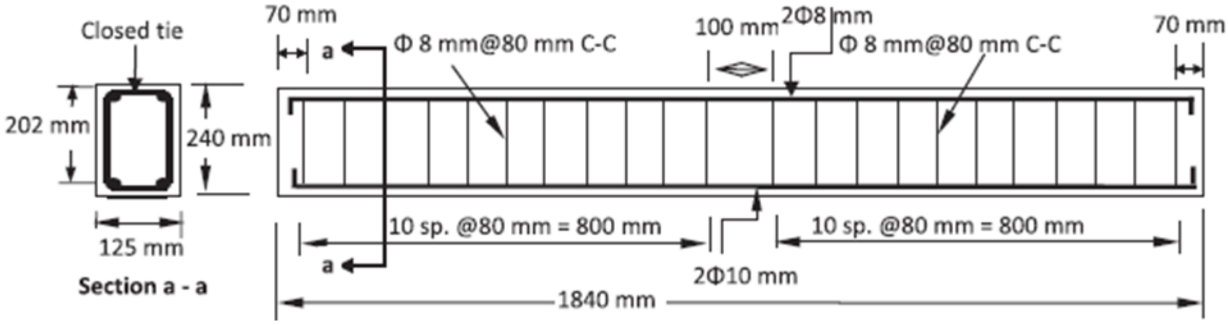

Figure 2-8: Simply supported beam detailing by Rami A. et al

Mahdi Arezoumandi et al (2015) conducted an experimental study on the flexural strength of reinforced concrete beams with 100% recycled concrete aggregate. Their work was an experimental investigation of the flexural strength of full scale reinforced concrete beams constructed with both 100% recycled concrete aggregate (RCA) as well as conventional concrete (CC). The test parameters for this study include longitudinal reinforcement ratio and concrete type. To conduct the research they use a simply supported beam reinforcement detailing as shown in Figure 2-9. The figure shows that the top reinforcement without anchorage or development length and the bottom reinforcement is with 90^{o} anchorage.

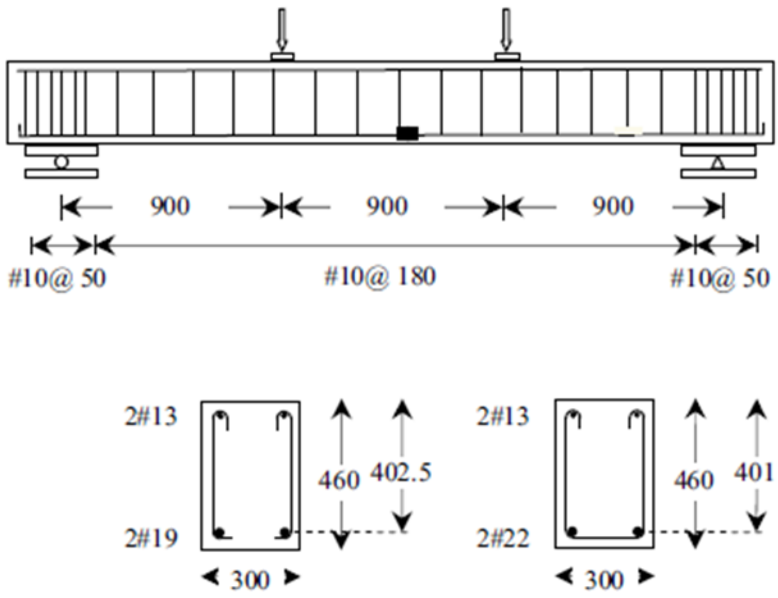

Figure 2-9: Simply supported beam detailing by Mahdi Arezoumandi et al

Sunil Raiyani and Sonal Thakkar (2017) studied to evaluate the behavior of reinforced concrete (RC) beam element under two-point loading with different pattern placement of tension reinforcement and its effect on ultimate load carrying capacity and deflection. They conclude that different pattern placement of tension reinforcement has an effect on load vs deflection diagram and cracking pattern of reinforced beam section. In their investigation, the reinforcement detailing of the test beam was shown in Figure 2-10. The detailing of the beam shows the longitudinal reinforcement is without anchorage or development length from the support.

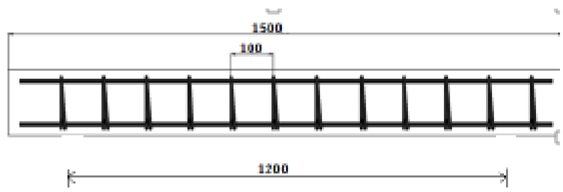

Figure 2-10: Simply supported beam detailing by Sunil Raiyani and Sonal Thakkar

Amith S. D. and H. B. Balakrishna (2015) in their experimental study on flexural behavior of reinforced concrete beam by partial replacement of fine aggregate with coal-based brick-kiln-ash, they used reinforcement detailing as shown in Figure 2-11. The longitudinal reinforcement detailing is the same as the detailing used by Sunil Raiyani and Sonal Thakkar.

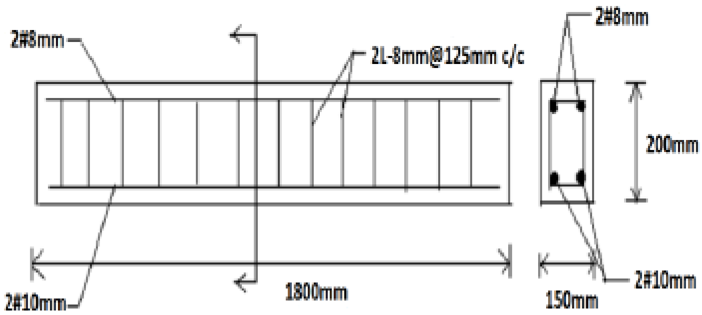

Figure 2-11: Simply supported beam detailing by Amith S. D. and H. B. Balakrishna

Arivalagan.S (2013) studied the flexural behavior of reinforced concrete beams as replacement of copper slag as fine aggregate and he uses the reinforcement detailing of a simply supported reinforced concrete beam as shown in Figure 2-12. The detailing of the beam shows that the longitudinal reinforcement both the tensile reinforcement and the compression reinforcement bars are with end anchorage.

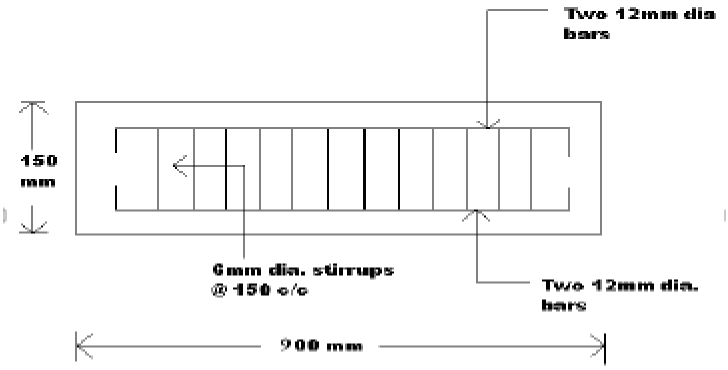

Figure 2-12: Beam reinforcement detailing by Arivalagan.S (2013)

2.6 Review Summary

A review of the literature shows that different researchers used different end anchorage of longitudinal reinforcement bar when studying about the strength of a beam. Some of the researchers provide 90^o end anchorage (development length) of the longitudinal reinforcement or provide development for the bar after the support in their experimental investigation. Other researchers, as we have seen in the literature review part, ignore the development of longitudinal reinforcement bars after the support even though Azlina et al. studies and confirm that a significant amount of tensile force exists in the support region due to the occurrence of the diagonal shear cracks. This suggests that longitudinal reinforcement in the shear span zone must be sufficiently extended into the support to avoid bond-splitting failure due to some shifting of the tensile force. In some cases, anchoring or developing of longitudinal reinforcement bars with 135^o from the support is a common practice, which is parallel to the shear cracks. This condition may increase the occurrence of shear crack and failure of the beam section before reaching the yield stress of the bar for shear critical beams.

In this research, the effect of providing development length with different anchorage angle on the shear and flexural strength of beams were studied.

CHAPTER 3 EXPERIMENTAL PROGRAM

3.1 Introduction

This chapter describes the experimental program completed at the Construction Materials Laboratory, Addis Ababa Institute of Technology (AAiT). Methods of specimen preparation from material characterization tests to test setup preparation were included in this chapter.

3.2 Concrete Ingredient Characterization

3.2.1 Cement

Types of cement available commercially in the market, OPC have been used for the study. The physical properties of the cement taken from the product standard. The specific gravity of the cement is 3.15.

3.2.2 Fine Aggregate (Sand)

Locally available Metehara washed sand passing through 4.75mm sieve was used. The material physical properties moisture content, silt content, specific gravity and gradation of the fine aggregate have been studied according to the recommended standard.

i. Gradation of aggregate

The particle size distribution of fine aggregate is shown in Table 3-1.

Table 3-1: Particle size distribution of sand AASHTO M 6-93 Or ASTM C 136

Weight of Sand	Sample (gm)				
	500				
AASHTO Sieve Size mm	Weight Retained	% Retained	% Pass	AASHTO M-6	
				Lower	Upper
9.5	0	0	100	100	100
4.75	15	3	97	95	100
2.36	19	3.8	93.2	80	100
1.18	40	8	84.2	50	85.0
0.600	130	26	59.2	25	60.0
0.300	225	45	14.2	10	30.0
0.150	61	12.2	2	2	10.0
0.075	7.6	1.52	0.4		
Pan	2.4	0.48	0		
Total sum	500	100		FM	2.49

Where: FM – Fines Modulus

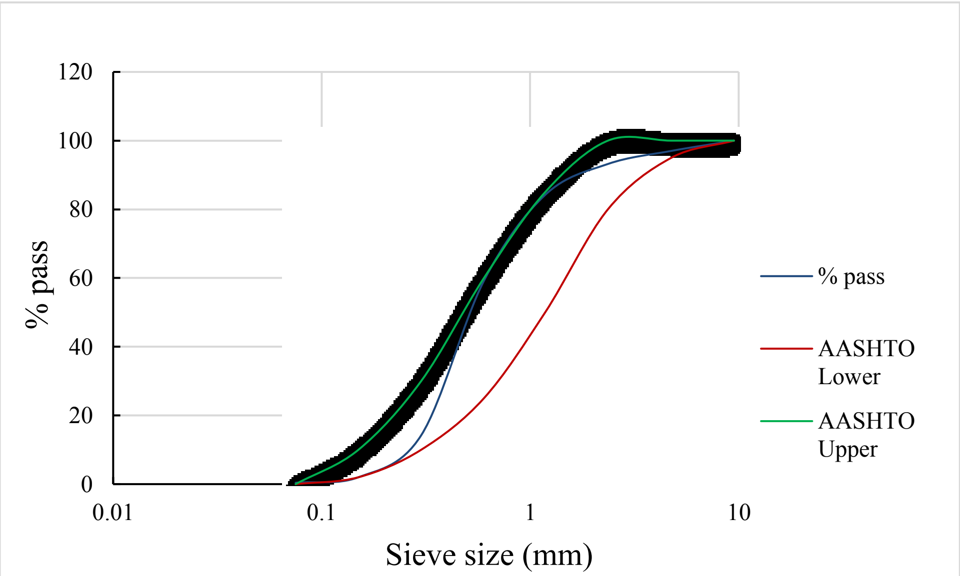

Figure 3-1: Gradation of fine aggregate

The gradation of the sample of sand used is within the upper and lower limit of the standard. It is, therefore, satisfactory to be used for concrete preparation. The physical properties of fine aggregate are summarized in Table 3-2.

ii. Properties of sand

Table 3-2: Physical properties of fine aggregate

Property of sand	Unit	Test value	Remark
Silt content	%	4.12	< 6%
Moisture content	%	3.3	
Specific gravity	-	2.52	
Absorption	%	1.8	
FM	-	2.49	
Unit weight	KN/m^3	1660.1	

3.2.3 Coarse Aggregate

Coarse aggregates used for specimen preparation were crushed aggregate. The size distribution of the coarse aggregate used in the study was shown in Table 4-3.

i. Sieve analysis of coarse aggregates

Table 3-3: Particle size distribution of coarse aggregate

AASHTO Sieve Size (mm)	Weight Retained (gm)	% pass of Aggregate	Specification ERA STS 8402-3		AASHTO M43-88	
			Lower	Upper	Lower	Upper
25	0	100	100	100	100	100
19.0	181.53	91	80	100	90	100
9.5	1371.56	23	10	40	20	55
4.75	463.91	0	0	4	0	10
Total	2017					

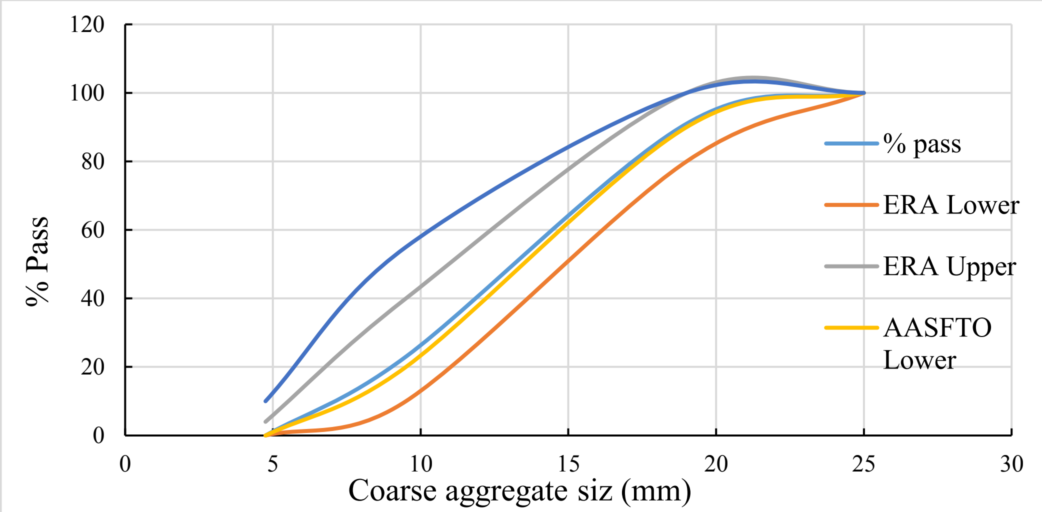

Figure 3-2: Coarse aggregate gradation

ii. Properties of coarse aggregate

Physical properties such as specific gravity, moisture content, and absorption of coarse aggregate were studied and the result was summarized in Table 4-3.

Table 3-4: Physical properties of coarse aggregate

Property of coarse aggregate	Unit	Test value	Remark
Moisture content	%	1.97	
Specific gravity	-	2.72	
Absorption	%	0.44	
Unit weight	KN/m^3	1687.2	

3.2.4 Water

Fresh and clean water which is free from organic matter, silt, oil, and acid material as per standard was used for casting and curing the specimen.

3.3 Plain Concrete

3.3.1 Concrete Composition

The composition of the constituent materials used in the investigation was summarized in Table 3-5 after the mix design was conducted.

Table 3-5: Composition of concrete

Materials	Weight (kg/m^3)	Ratio
Cement	332.79	1
Fine aggregate	714.99	2.15
Coarse aggregate	1100.05	3.31
Water	172.91	0.52
Unit wet of concrete	2350.88	

3.3.2 Fresh Properties of Concrete

During the preparation of test spacemen's, the same type of concrete (the same material composition) is used. But the mix was prepared three times. The slump values of each mix were taken. Slump value test procedures shown in Figure 3-3.

Figure 3-3: Slump value test

To determine the mechanical properties of plain concrete, cubes specimen for compressive strength and cylinder specimens for tensile strength were cast. Figure 3-4 shows concrete mixing and also cube & cylinder specimens preparation.

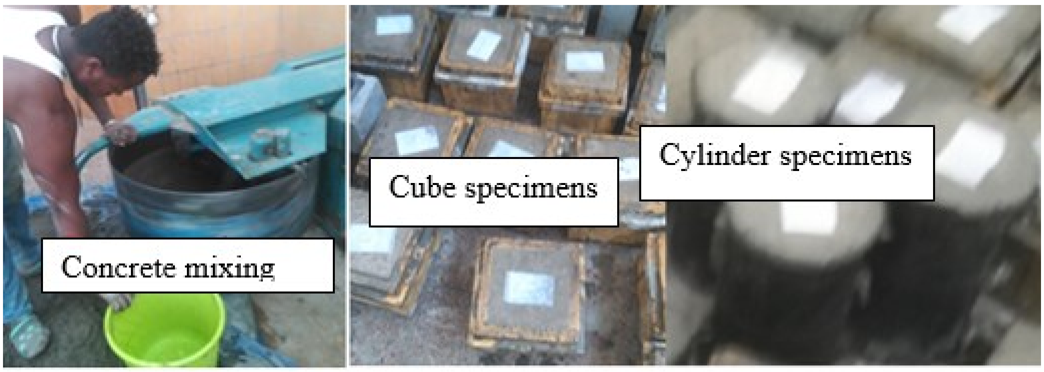

Figure 3-4: Mixing and molding of test specimens

3.3.3 Harden Properties of Concrete

i. Compressive strength.

The compressive strength of concrete was investigated using a universal testing machine. The cube compressive strength of plain concrete was determined using the Universal Testing Machine shown in Figure 3-5.

Figure 3-5: Universal concrete compressive testing machine

ii. Tensile strength

The tensile strength of concrete is one of the basic and important properties which greatly affect the extent and size of cracking in structures. Moreover, the concrete is very weak in tension due to its brittle nature. So, concrete develops cracks when tensile forces exceed its tensile strength.

Therefore, it is necessary to determine the tensile strength of concrete to determine the load at which the concrete members may crack. Furthermore, splitting the tensile strength test on a concrete cylinder is a method to determine the tensile strength of concrete. Figure 3-6 shows the tensile splitting test cylinder specimens and testing machines.

Figure 3-6: Tensile Strength Test Specimens

The tensile strength was calculated using equation (3-1).

$$\mathbf{T} = \frac{\mathbf{2P}}{\pi \mathbf{LD}} \qquad \textbf{(3-1)}$$

Where:

T = splitting tensile strength, MPa

P = maximum applied load indicated by the testing machine, N

D = diameter of the specimen, mm

L = length of the specimen, mm

3.4 Reinforcement Steel

In the preparation of experimental beam specimens, plain reinforcement bar with a diameter of 6 mm bar was used as shear reinforcement for shear critical beams. 8 mm deformed bar was used as negative reinforcement for all specimens and as shear reinforcement for specimens fails in flexure. Three beams, specimen's weak in flexure, were cast with 10mm reinforcement steel as bottom reinforcement bars and the rest were cast using a 20mm reinforcement bar as bottom reinforcement. The grade of reinforcement bars is $S_{500.}$ The reinforcement test was conducted in Addis Ababa university AAiT Laboratory UTM machine. Figure 3-7 shows the reinforcement testing machine used in AAiT.

Figure 3-7: Steel reinforcement testing machine

3.5 Beam Specimens

3.5.1 Details of Specimens

The experimental program consists of 6 simply supported RC beam specimens with rectangular cross-section. Three of them are with constant width (B) and depth (D) of 150 mm and 200 mm respectively. The rest are with constant width (B) and depth (D) of 200 mm and 250 mm respectively. Table 3-6 summarizes the detailing of beam specimens.

Table 3-6: Details of experimental sample beams

Speci men's	Width (mm)	Total depth (mm)	Effective depth (mm)	Concrete cover (mm)	Longitudin al rebar (mm^2)	Anchorage & development length of bars from the support
THB-1	150	200	162	25	157	Development with 90^o anchorage
THB-2	150	200	162	25	157	Development with 135^o anchorage
THB-3	150	200	162	25	157	Without development from the support
THB-4	200	250	209	25	942	Development with 90^o anchorage
THB-5	200	250	209	25	942	Development with 135^o anchorage
THB-6	200	250	209	25	942	Without development from the support

The details of the flexure critical and shear critical beam details shown in Table 3-6 are shown in Figure 3-8 and Figure 3-9 respectively.

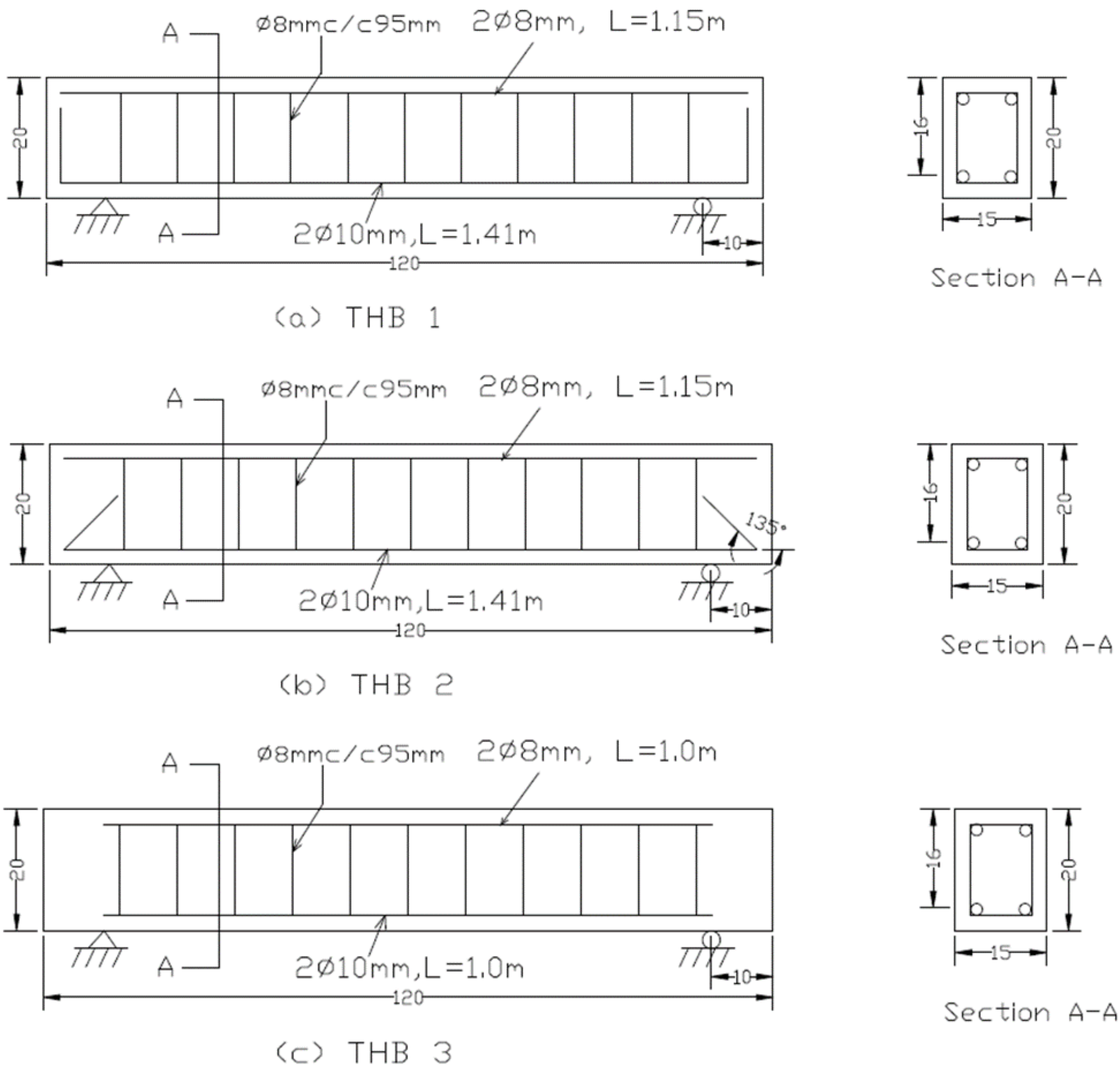

Figure 3-8: Flexural beam specimens detailing

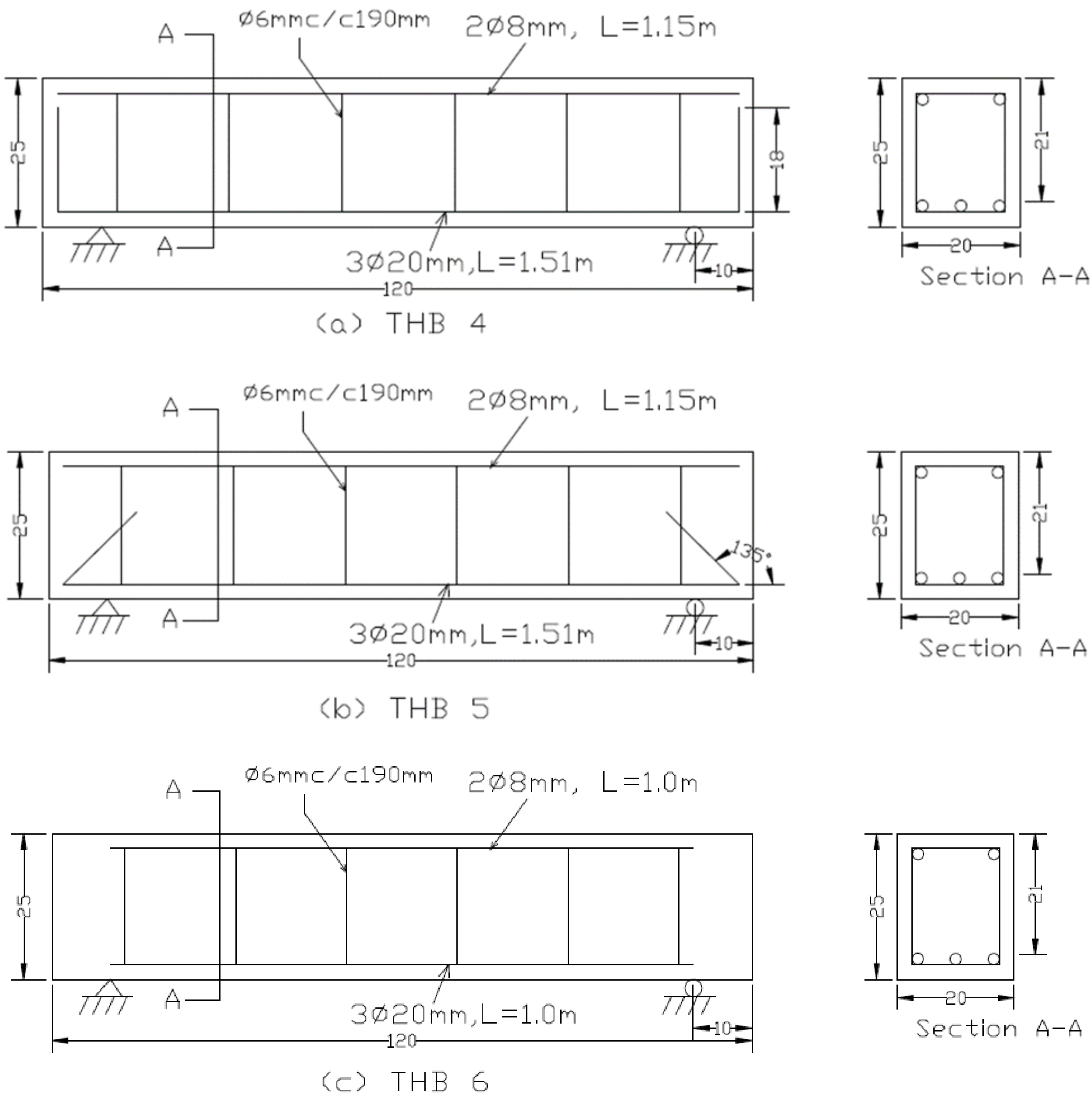

Figure 3-9: Shear beam specimens detailing

3.5.2 Specimen Preparation

The test specimens were constructed at the AAiT Construction Materials Laboratory. The formworks were prepared from timber and steel reinforcement was prepared according to the specified detailing. The specimens were cast in the laboratory and vibrator was used to consolidate the concrete. Reinforced concrete beam specimens casting and compaction process is shown in Figure 3-10.

Figure 3-10: Formwork preparation and specimen casting

3.5.3 Curing and Demolding

Curing plays an important role in strength development and durability of concrete. So curing takes place immediately after concrete placing and finishing, and involves maintenance of desired moisture and temperature conditions, both at depth and near the surface. During the curing process adequate amount of moisture was provided for continues hydration and development of strength. The curing and demolding process is shown in Figure 3-11.

Figure 3-11: Specimens curing and removal of formworks

3.6 Testing Tools Used in Beam Manual Test

The test setup was prepared manually in AAiT construction material laboratory. The test specimens were beam section and a point loading test was conducted. In the preparation of the test setup the following tools; applied load measuring load cell, deflection measuring transducer, hydraulic jack which applies load and data logger for recording of the whole data were used. The instruments used in the test setup were shown in Figure 3-12.

Figure 3-12: Specimen testing tools

CHAPTER 4 FINITE-ELEMENT ANALYSIS

4.1 Introduction

Finite element analysis software available from the University of Toronto for the prediction of reinforced concrete elements was used to predict the shear strength and flexural strength behavior of beams. In the following section, a brief description of procedures taken to model beam specimens on VecTor2 software is presented. A more detailed description of the software can be found in the VecTor2 and FormWorks User's Manual (Wong and Vecchio, 2002).

4.2 Models for Concrete Materials

The concrete constitutive and behavioral models are paramount to the accuracy of the VecTor2 results. At each load step, the structure stiffness is determined from the stresses and strains calculated from the constitutive models. Further, the inclusion or omission of a model determines whether the effects of pertinent behaviors are included in the analysis, and the suitability of the results to the purpose of the analysis. Many of the models in VecTor2 include multiple options differing in degree and type, which may produce a divergence of results.

4.2.1 Compression Pre-Peak Response

In the analysis of the compression pre-peak response, the Hognestad parabola was used. The Hognestad parabola, as shown in Figure 4-1, is a simple compression response curve.

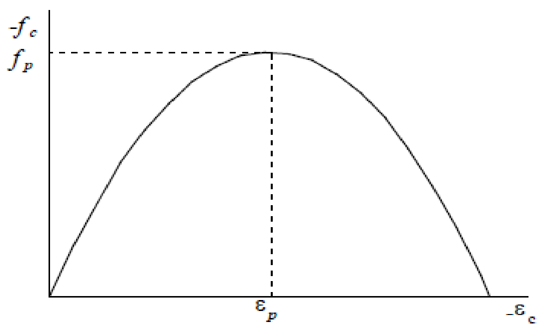

Figure 4-1: Hognestad parabolic pre- and post-peak concrete compression response

The stress-strain curve is described by the following relationship:

$$\mathbf{f_{ci}} = -\mathbf{f_p}\left\{2\left(\frac{\varepsilon_{ci}}{\varepsilon_p}\right) - \left(\frac{\varepsilon_{ci}}{\varepsilon_p}\right)^2\right\} < 0 \quad \textbf{for } \varepsilon_{ci} < 0 \qquad \textbf{(4-1)}$$

Where: f_{ci} = Principal compressive stress

f_p = Peak compressive stress

ε_p = Peak strain

ε_{ci} = Principal compressive strain

The stress-strain relationship is symmetric about ε_p, diminishing to zero stress at zero strain and $2\varepsilon_p$. The Hognestad parabola predefines the initial tangent stiffness, E_c, as follows:

$$\boldsymbol{E_c = 2\,f_p/|\varepsilon_p|} \qquad \textbf{(4-2}$$

Where: E_c = Concrete stiffness

4.2.2 Compression Post-Peak Response

Beyond the peak compressive stress, f_p, and corresponding strain, ε_p, concrete resists substantial compressive stress under continued compressive straining. Moreover, confinement of the concrete by transverse stresses enhances the strength and ductility of the concrete, transforming the failure in compression from brittle to ductile. This residual compressive strength and ductility may allow localized regions of a reinforced concrete structure to fail, but gradually unload so as to redistribute internal stresses and forestall total failure of the structure until additional deformation occurs. Compression post-peak response models compute the principal compressive stress, f_{ci}, if the compressive principal compressive strain, ε_{ci}, is more compressive than the strain, ε_p, corresponding to the peak compressive stress, f_p. The peak parameters are determined by adjusting the unconfined uniaxial concrete cylinder strength, f'_c, and the corresponding strain, ε_o, for compression softening due to transverse tensile strains, and strength enhancement due to confinement.

In the simulation process, the Modified Park-Kent model was used as a compression post-peak response in the modeling of reinforced concrete beam specimens.

4.2.3 Compression Softening

Compression softening in cracked concrete is the reduction of compressive strength and stiffness, relative to the uniaxial compressive strength, due to coexisting transverse cracking and tensile straining. This reduction can be substantial and have considerable effects on the load-deformation response of reinforced concrete structures, in terms of stiffness, ultimate strength capacity, and ductility.

Strength-and-strain softened models, as shown in Figure 4.2, use β_d to reduce both the uniaxial compressive strength, f'_c, and corresponding strain, ε_o, to determine the peak compressive strength, f_p, and corresponding strain, ε_p, used in the compression response models. The value of β_d is a function of $\varepsilon_{c1}/\varepsilon_{c2}$, the ratio of the principal tensile strain to the principal compressive strain.

In this work, Vecchio 1992-A (e1/e2-Form) model was used to account for concrete compression softening. The model was shown in Fig 4.3.

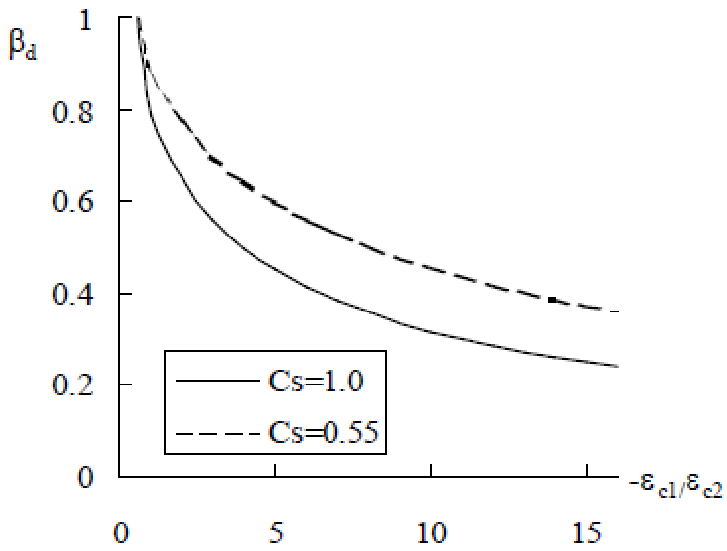

Figure 4-2: Vecchio 1992-A compression softening model

4.2.4 Tension Stiffening

In tension, concrete is predominantly brittle and its response can be differentiated into an uncracked and cracked response. After cracking in reinforced concrete structures, the concrete tensile stresses diminish virtually to zero at the free surface of cracks. However, owing to bond action with the reinforcement, average concrete tensile stresses continue to exist in the concrete between the cracks in the vicinity of the reinforcement. With additional tensile straining, cracks widen, the bond action degrades near the cracks and the average concrete tensile stresses gradually diminish to zero.

To account for this behavior of concrete Modified Bentz 2003 was used. The Bentz 2003 formulation for tension stiffening incorporates the percentage of reinforcement as well as bond characteristics.

4.2.5 Tension Softening

Tension softening refers to the presence of post-cracking tensile stresses in plain concrete. Under increased tensile straining, the tensile stresses diminish to zero. This phenomenon is attributable to the fact that concrete is not perfectly brittle. Rather, as described by fracture mechanics approaches, the formation of a localized crack requires energy. As the fracture process progresses and the crack widens, concrete in the vicinity of the crack is gradually relieved of stress, and the dissipated energy propagates the crack tip.

In this simulation, the linear tension softening model was used. The tension softening base curve descends linearly from the cracking stress and strain to zero stress at the characteristic strain (i.e. the terminal strain is taken as the characteristic strain).

$$\boldsymbol{f_{ts,base} = f_{cr}\left[1 - \frac{(\varepsilon_{c1}-\varepsilon_{cr})}{(\varepsilon_{ch}-\varepsilon_{cr})}\right] \geq 0 \quad for\ \varepsilon_{cr} < \varepsilon_{c1}} \qquad \textbf{(4-3)}$$

Where: $f_{ts,base}$ =

ε_{c1} = Principal tensile strain

ε_{cr} = Cracked strain

ε_{ch} = Characteristics strain

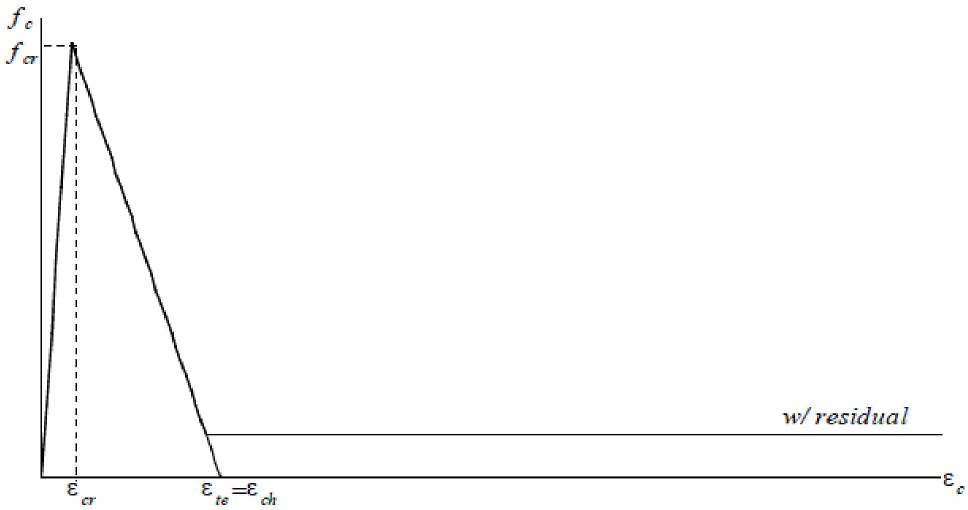

Figure 4-3: Linear tension softening response with and without residual

4.3 Material Properties for Modelling

The mechanical properties of concrete, the compressive strength and tensile strength found from the experimental result and steel reinforcement mechanical properties result found from the experimental investigation were used in the modeling of specimens.

4.4 Specimen Modeling on Vector 2

A total of six beams were modeled on Vector 2 finite element analysis software. The condition of the analysis was nonlinear to account for the actual behavior of reinforced concrete. In the preparation of specimens, the same cross-sections and reinforcement arrangement of beams and the same support condition and load plate was used. From the total six beams, three of them fail in flexure and the others fail in shear like that of experimental investigation. In the modeling of specimens 25mm x 25mm mesh size was used for the whole reinforced concrete beam specimens.

4.4.1 Models of Flexure Critical Beams

Three flexure critical beams were modeled in VecTor2 software based on longitudinal reinforcement bar end anchorage arrangement as shown in Figure 4-5.

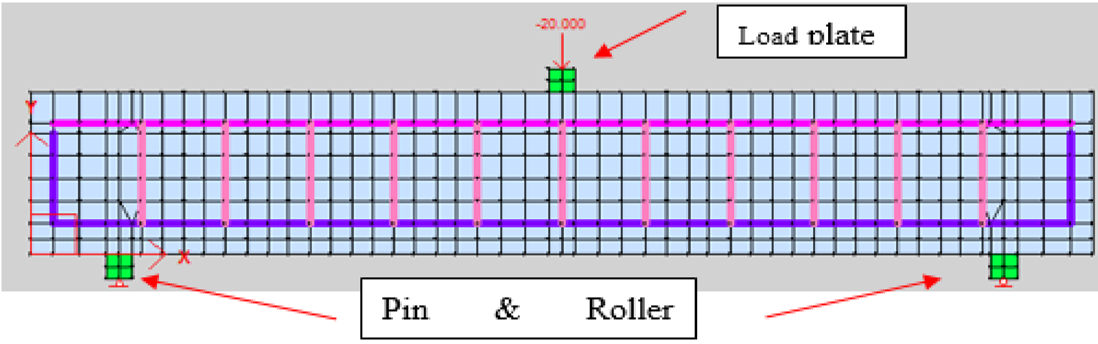

a) THB-1 Vector 2 model

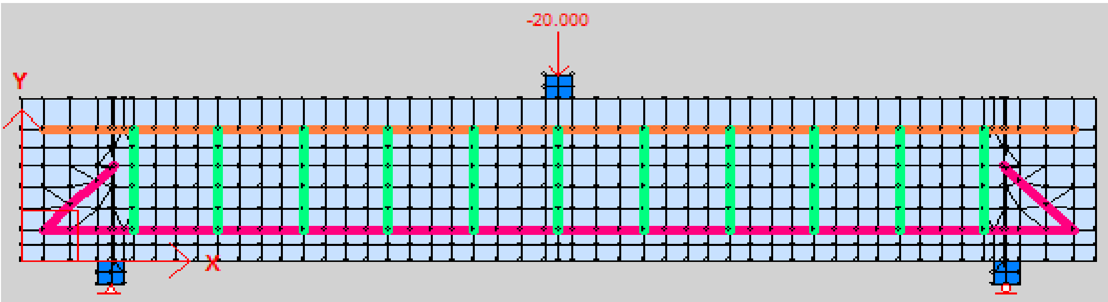

b) THB-2 Vector 2 model

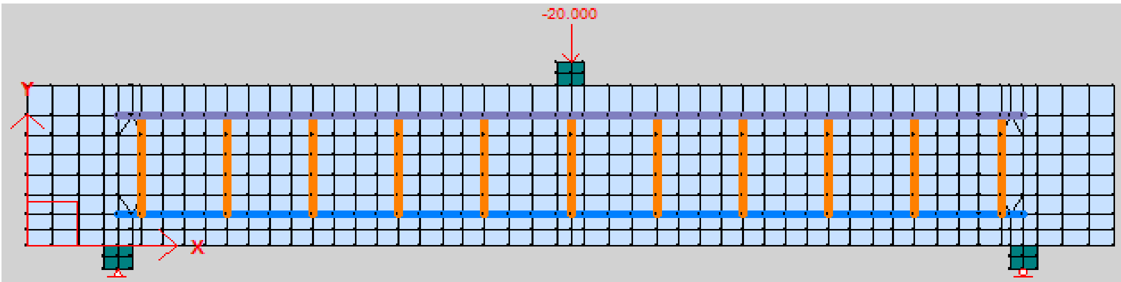

c) THB-3 Vector 2 model

Figure 4-4: Models of flexure beams on vector

4.4.2 Models of Shear Critical Beams

Three shear critical beams were modeled in VecTor2 software based on longitudinal reinforcement bar end anchorage arrangement as shown in Figure 4-6.

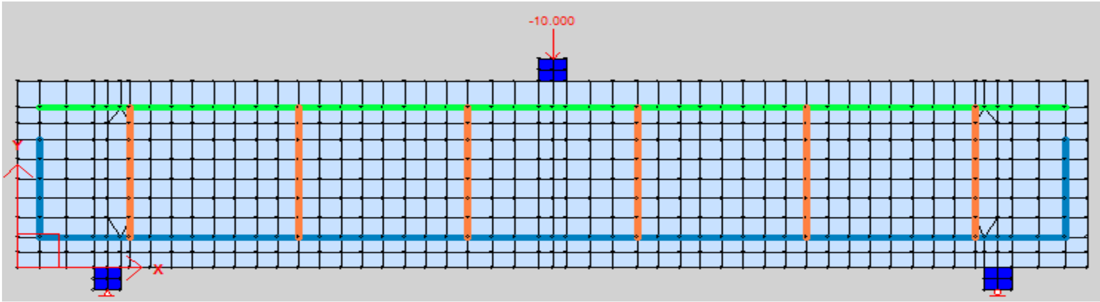

a) THB-4 Vector 2 model

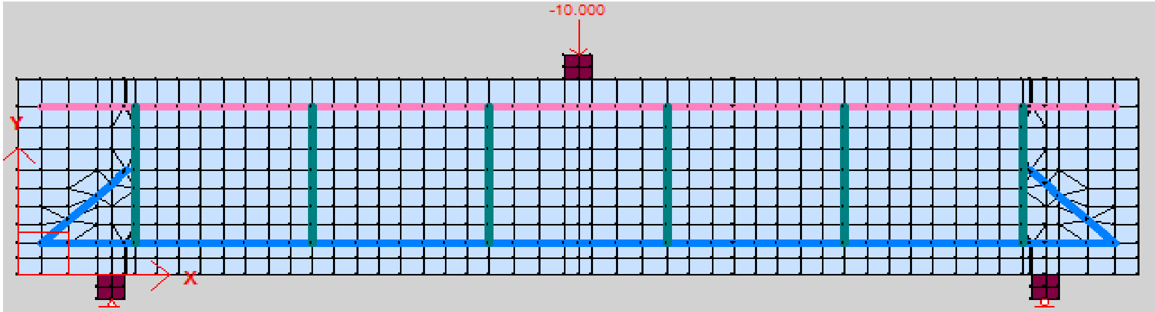

b) THB-5 Vector 2 model

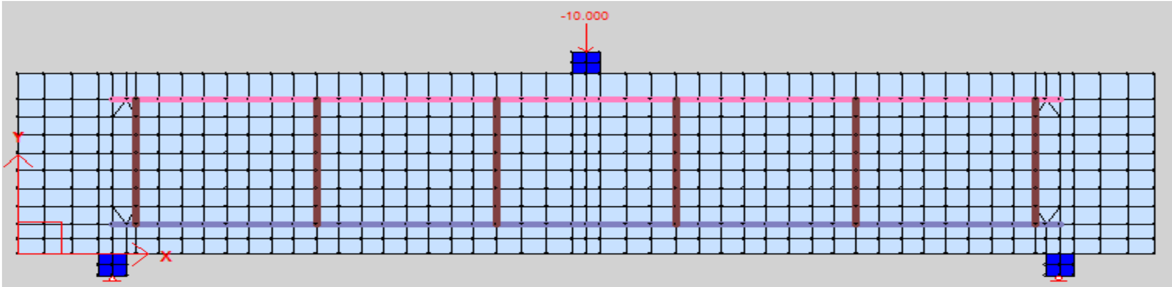

c) THB-6 Vector 2 model

Figure 4-5: Models of shear beams on vector

CHAPTER 5 RESULT AND DISCUSSION

5.1 Introduction

This chapter focuses on the test results found from the experiment and FEA. Its main concern is two parts. The first part focuses on the mechanical properties of plain concrete and reinforcement steel, which are compressive and tensile strength of plain concrete and tensile properties of steel reinforcement. The second part provides a detailed analysis of the flexure and shear critical reinforced concrete beams resistance capacities. The investigation mainly focusses on the behavior of the reinforced concrete beams by reviewing load versus deflection diagram, crack pattern, flexural and shear strength and failure mode.

5.2 Mechanical Properties of Plain concrete & Reinforcing Steel

5.2.1 Properties of Plain Concrete

Slump values, cube compressive strength values and tensile strength values for each mix determined in AAiT laboratory are shown in the following sections.

5.2.1.1 Slump Value of Concrete

The slump values of the concrete mix are shown in Table 5-1.

Table 5-1: Slump values of concrete mix

Mix No	Mix used	Slump value (mm)
Mix 1	For THB-1 & THB-2	39
Mix 2	For THB-3 & THB-6	42
Mix 3	For THB-4 & THB-5	46

As Table 5-1 shows, the slump value of each mix has within the recommended maximum and minimum values of (ACI-2111_91) and approximately comparable values.

5.2.1.2 Compressive Strength of Plain Concrete

The cube compressive strength of the concrete mix is shown in Table 5-2.

Table 5-2: Compressive strength cube test result

Mix No	Mix used	Day-7 compressive strength (MPa)	Day-28 compressive strength (MPa)	A beam's testing day (MPa)
Mix-1	For THB-1 & THB-2	23.25	36.01	36.11
Mix- 2	For THB-3 & THB-6	22.82	36.56	36.45
Mix- 3	For THB-4 & THB-5	23.35	35.43	35.85

5.2.1.3 Tensile Strength of Plain Concrete

The tensile splitting test results of plain concrete are shown in Table 5-3.

Table 5-3: Tensile strength test result

Mix No	Mix used	Concrete tensile strength (MPa)
Mix-1	For THB-1 & THB-2	2.14
Mix-2	For THB-3 & THB-6	2.32
Mix-3	For THB-4 & THB-5	1.87

5.2.2 Properties of Steel Reinforcement

The mechanical properties of reinforcement steel used as concrete reinforcement material is shown in Table 5-4.

Table 5-4: Reinforcement material test result from AAiT laboratory

Specimen No	Diameter		Yield Load [kN]	Failure Load [kN]	Yield capacity [MPa]	Ultimate capacity [MPa]	Elongat ion [%]	Length [cm]
	D1,[mm]	D2,[mm]						
ϕ_6-1	5.35	-	9.2	12.6	325.55	445.86	23.9	80
ϕ_6-2	5.34	-	9.1	13.9	322.01	491.86	23.8	80
ϕ_6-3	5.33	-	9.3	13.2	329.09	467.10	23.9	80
Average					**325.55**	**468.27**		
ϕ_8-1	7.43	8.58	27.47	33.78	546.72	672.45	23.7	80
ϕ_8-2	7.41	8.60	27.26	34.01	542.68	676.91	23.5	80
ϕ_8-3	7.45	8.62	27.05	34.40	538.42	684.65	23.8	80
Average					**542.61**	**678.00**		
ϕ_{10}-1	9.44	10.56	42.9	54.2	546.50	690.45	23.7	80
ϕ_{10}-2	9.46	10.58	43.8	54.7	557.96	696.82	23.6	80
ϕ_{10}-3	9.42	10.58	44.1	54.6	561.78	695.54	23.7	80
Average					**555.41**	**694.27**		
ϕ_{20}-1	19.40	20.72	204.2	223.2	650.32	710.83	23.6	80
ϕ_{20}-2	19.44	20.74	198.6	223.5	632.48	711.78	23.7	79
ϕ_{20}-3	19.42	20.72	200.5	223.8	638.54	712.74	23.6	80
Average					**640.45**	**711.78**		

5.3 Flexure Critical Beam Investigation Results

Three types of six beams (weak in flexure) were studied based on different longitudinal reinforcement end anchorage. Three of them were studied experimentally and the others were using FEA simulation VecTor2 software, to compare with the experimental result. In all the six specimens, a typical flexural failure mechanism was observed. The result and discussion are shown in the following sections.

5.3.1 Flexure Critical Beams Crack Pattern

5.3.1.1 Experimental Flexure Critical Beams Crack Pattern

The experimental crack patterns of flexure critical beams are shown in Figure 5-1 to Figure 5-3.

Figure 5-1: Experimental flexure failure crack patterns of THB-1

Figure 5-2: Experimental flexure failure crack patterns of THB-2

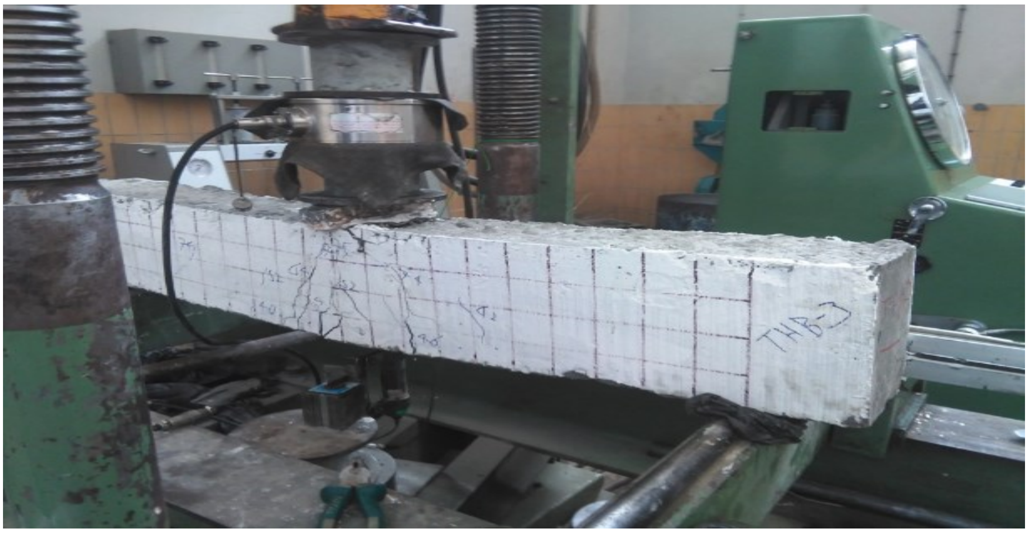

Figure 5-3: Experimental flexure failure crack patterns of THB-3

The above figures, Figure 5-1 to Figure 5-3 show approximately the same flexural failure crack patterns.

5.3.1.2 FEA Flexure Critical Beams Crack Pattern

The beams tested in the experiment also analyzed using finite element software (FEA). The crack pattern simulation results of the beams are shown in the following figures, (Figure 5-4 to Figure 5-6).

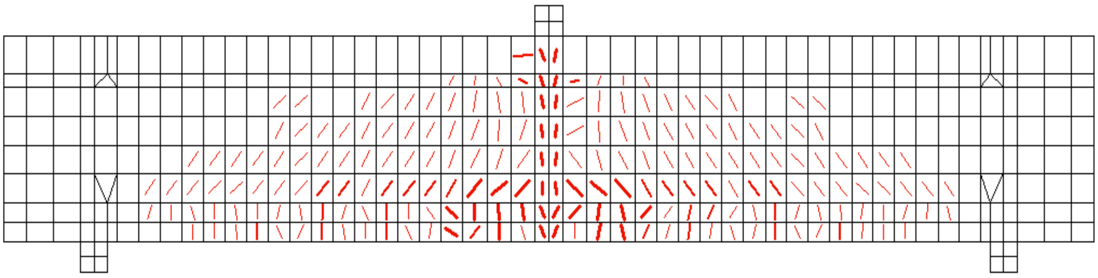

Figure 5-4: FEA flexure failure crack patterns of THB-1

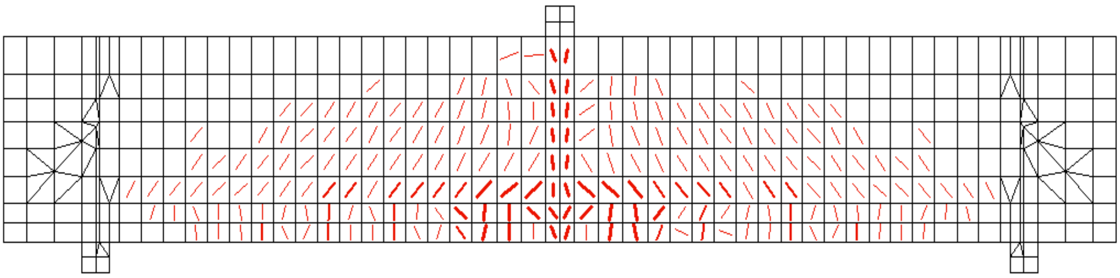

Figure 5-5: FEA flexure failure crack patterns of THB-2

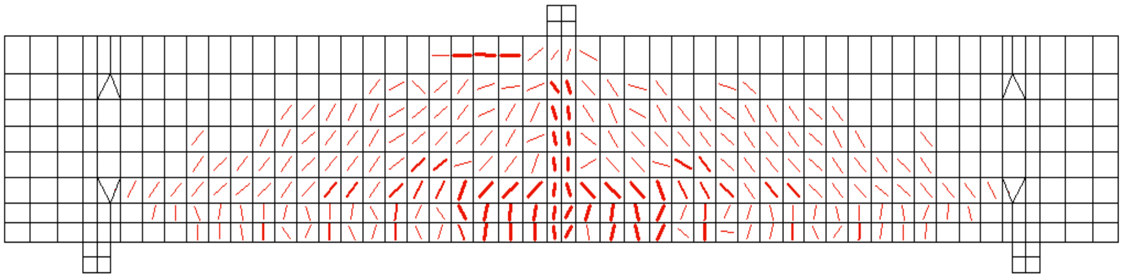

Figure 5-6: FEA flexure failure crack patterns of THB-3

Likewise the experimental result, the finite element analysis result gives approximately the same flexure failure crack patterns for THB-1, THB-2, and THB-3.

5.3.1.3 Experimental & FEA Crack Pattern Comparison of Flexure Critical Beams

The experimental and finite element analysis crack pattern comparison is summarized as follows.

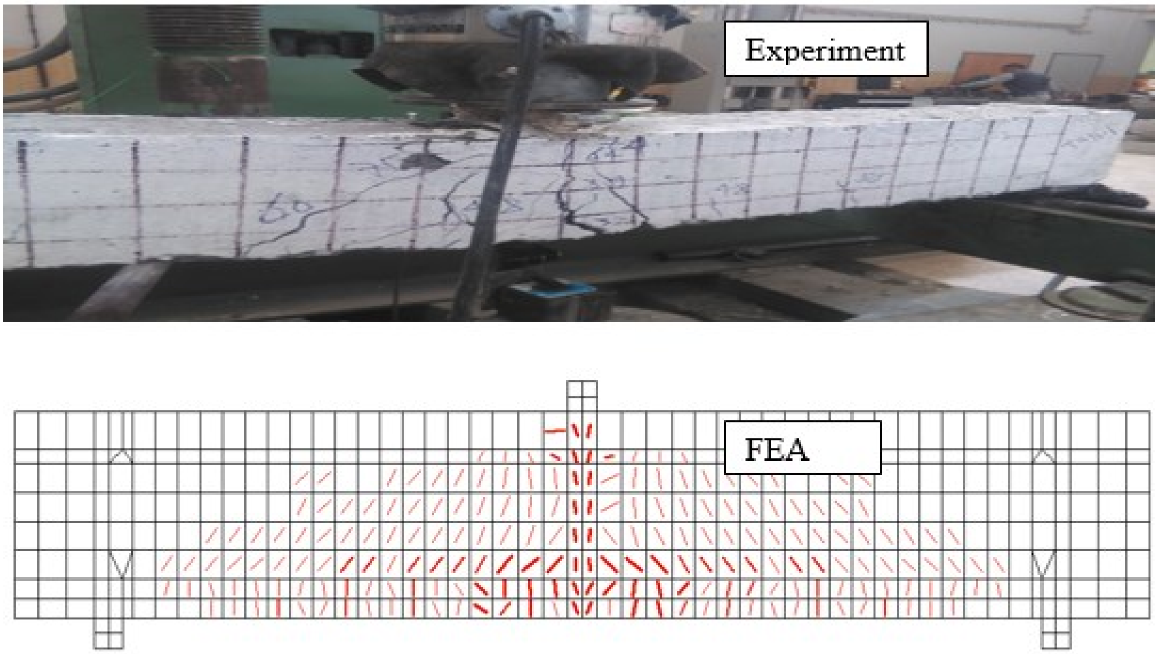

Figure 5-7: Flexural failure crack patterns of THB-1

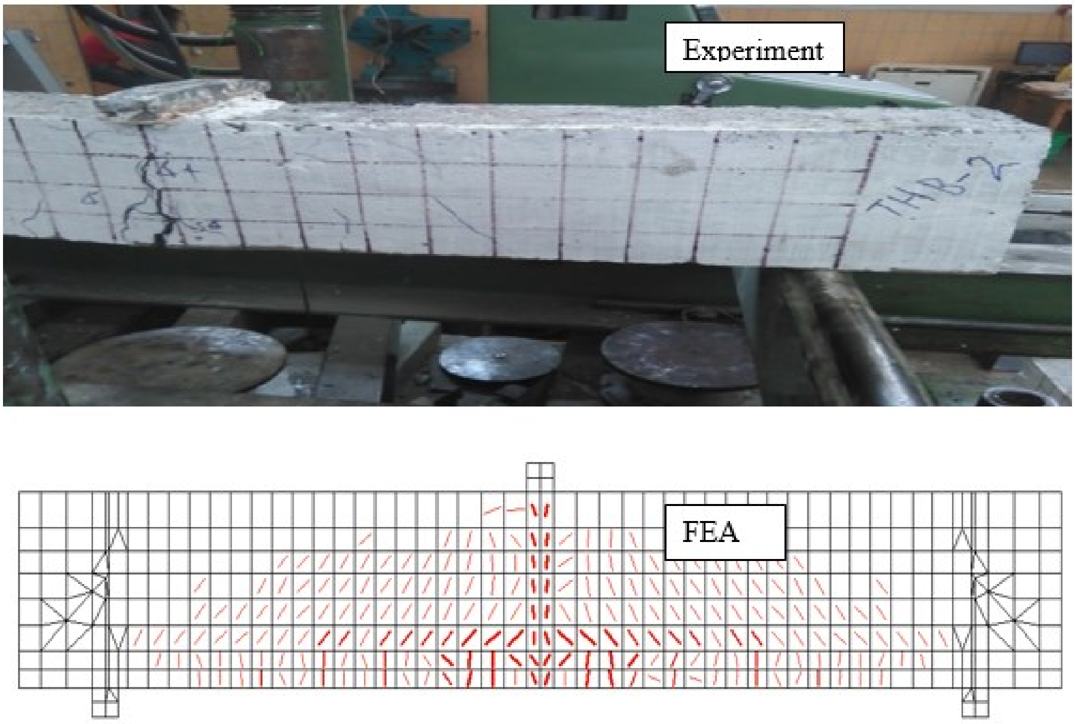

Figure 5-8: Flexural failure crack patterns of THB-2

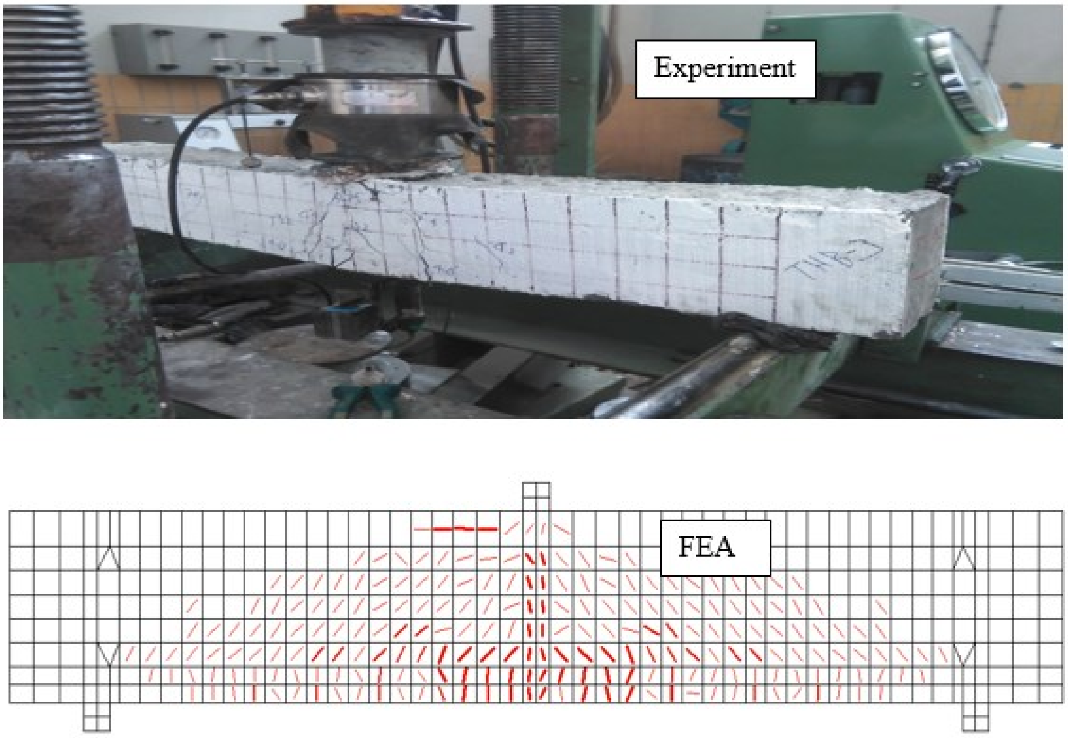

Figure 5-9: Flexural failure crack patterns of THB-3

The experimental and the FEA simulation result give comparable flexural crack patterns for each beam as shown in Figure 5-7 to Figure 5-9.

5.3.1.4 Flexure Critical Beams Comparison Based on Crack Patterns

The above figures, Figure 5-7 to Figure 5-9 show that the experiment and also the FEA crack patterns of flexure critical beams (THB-1, THB-2, and THB-3). The crack patterns of the three beams seem to be the same. This indicates that providing development length and different anchorage angle to the tensile longitudinal reinforcement bars further from the support have no significant effect on flexure critical beams crack pattern.

5.3.2 Load vs Deflection Diagrams of Flexure Critical Beams

5.3.2.1 Experimental Load Vs Deflection Diagram of Flexure Critical Beams

The experimental load vs deflection diagrams of the three flexure critical beams are shown in Figure 5-10 to Figure 5-12.

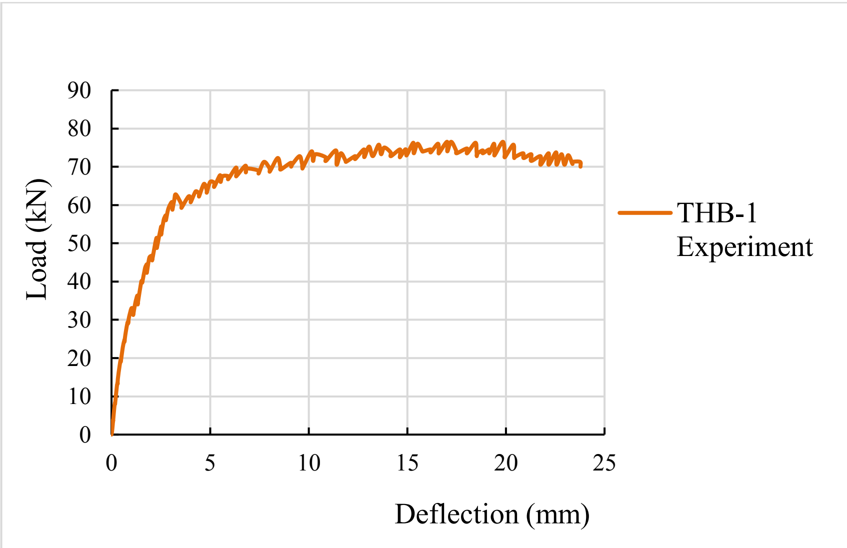

Figure 5-10: Experimental load vs deflection diagram of THB-1

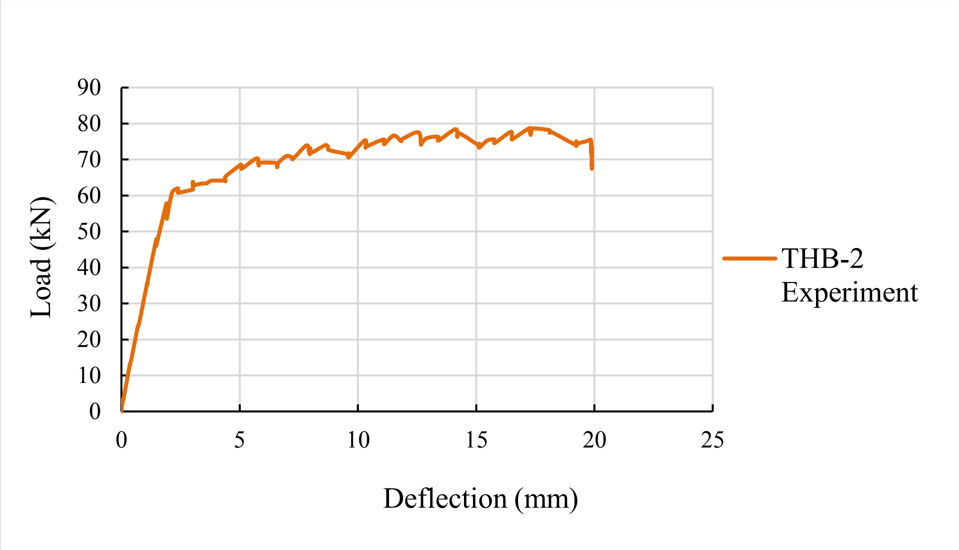

Figure 5-11: Experimental load vs deflection diagram of THB-2

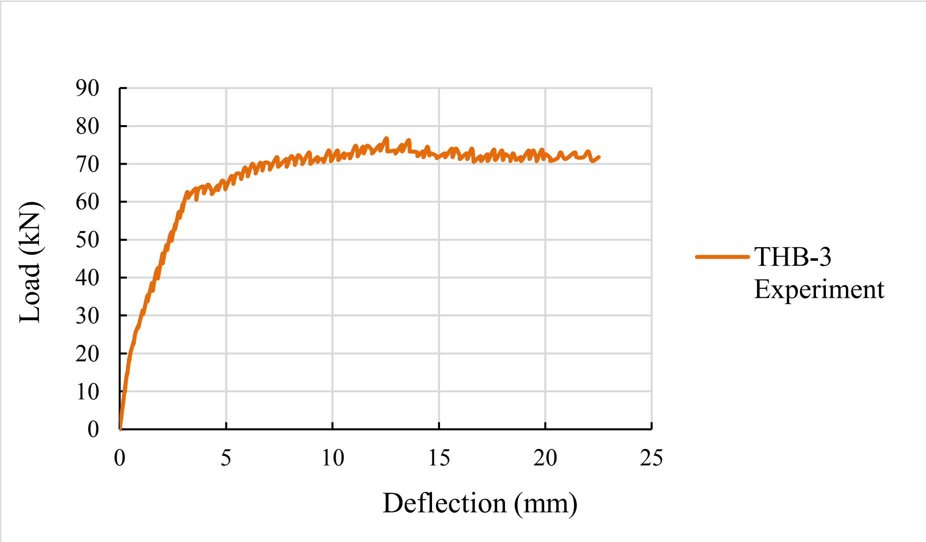

Figure 5-12: Experimental load vs deflection diagram of THB-3

From the above experimental load vs deflection diagrams the ultimate load for the beams, THB-1, THB-2, and THB-3 are 77.01kN, 78.76kN and 76.78kN respectively.

5.3.2.2 FEA Load Vs Deflection Diagram of Flexure Critical beams

The simulation results of flexure critical beams load vs deflection diagram are shown in Figure 5-13 – Figure 5-15. The figures show that the FEA ultimate loads of THB-1, THB-2, and THB-3 are 72.85kN, 73.78kN and 76.09kN respectively.

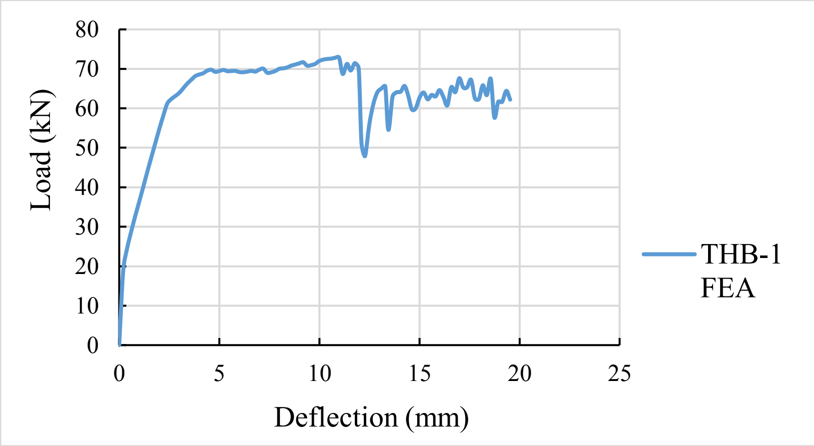

Figure 5-13: FEA Load vs deflection diagram of THB-1

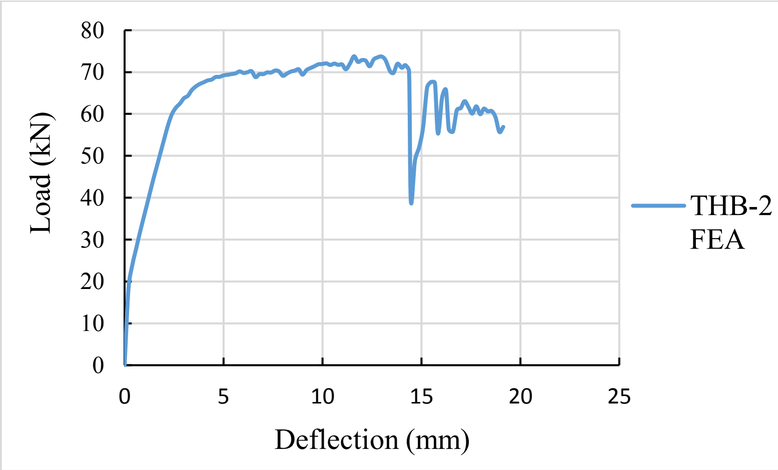

Figure 5-14: FEA Load vs deflection diagram of THB-2

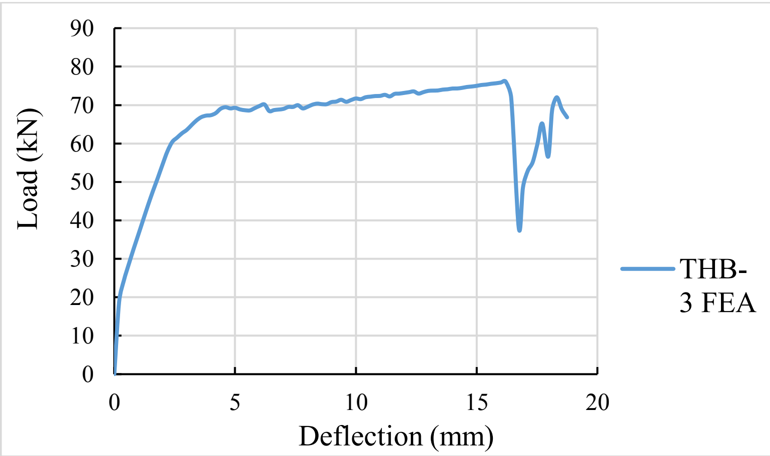

Figure 5-15: FEA Load vs deflection diagram of THB-3

5.3.2.3 Experimental & FEA Load vs Deflection Diagram Comparison

Figure 5-16 to figure 5-18 briefly describes the comparison between the experimental and the FEA load vs deflection diagrams of THB-1, THB-2, and THB-3.

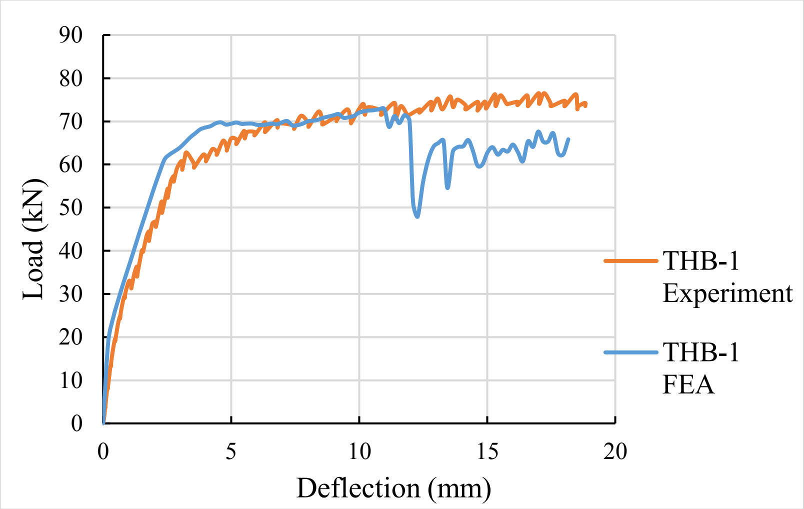

Figure 5-16: Load vs deflection diagram of THB-1

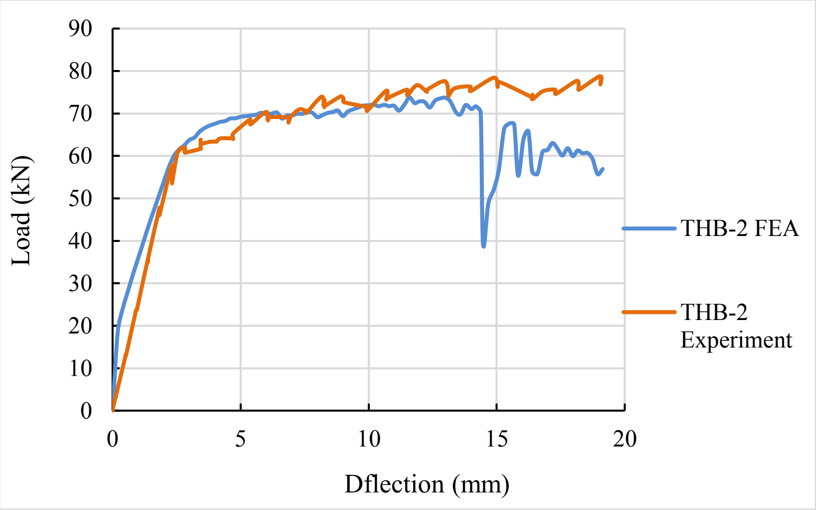

Figure 5-17: Load vs deflection diagram of THB-2

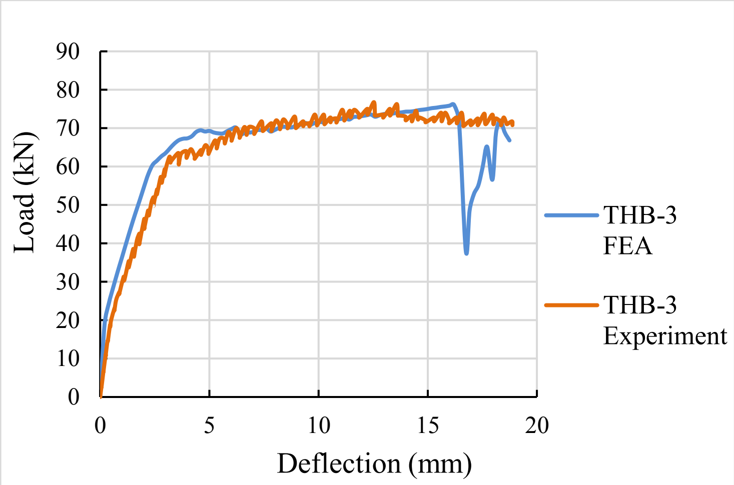

Figure 5-18: Load vs deflection diagram of THB-3

The experiment and FEA load vs deflection results of the flexure critical beams gives nearly the same load vs deflection diagram for each beam.

5.3.2.4 Flexure Critical Beams Comparison Based on Load Vs Deflection Diagram

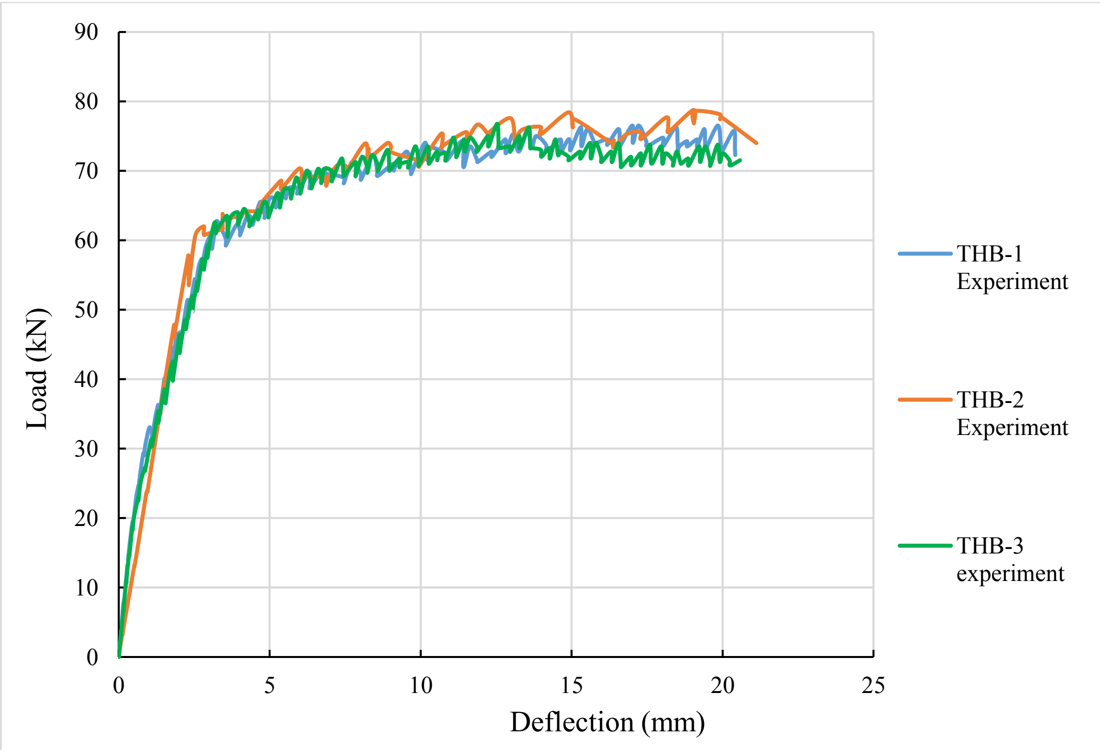

Figure 5-19: Experimental load vs deflection diagram of flexure beams

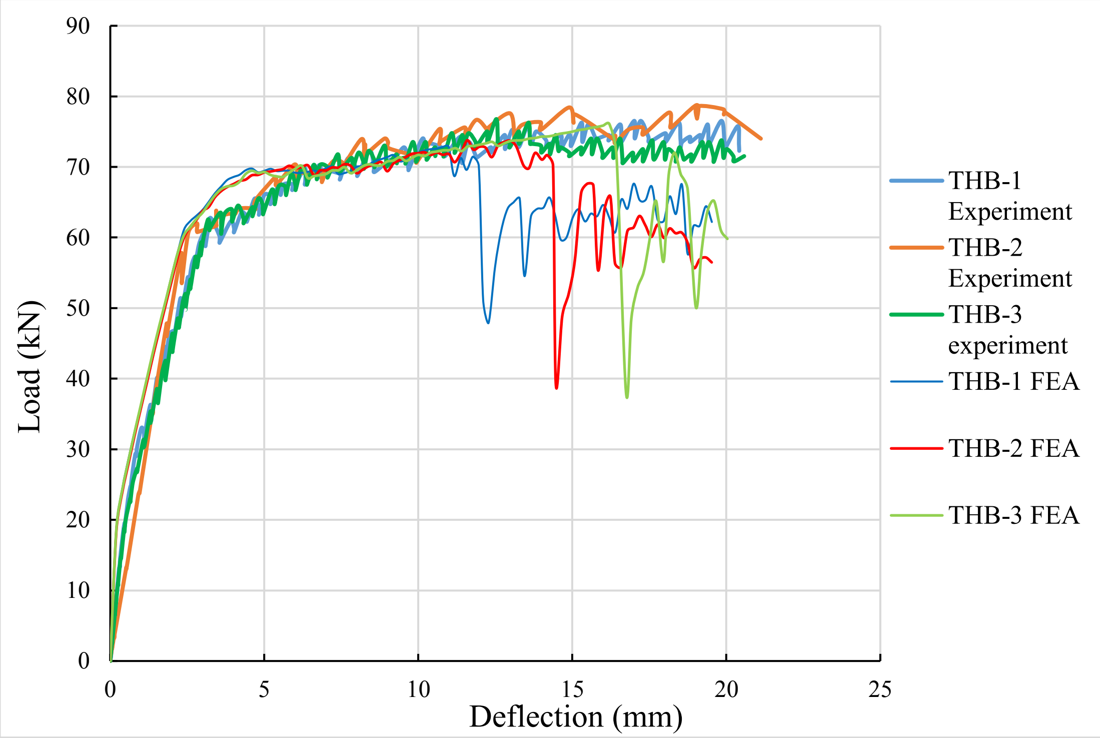

Figure 5-20: Experimental & FEA load vs deflection diagram of flexure beams

The result in Figure 5-20 shows that the load vs deflection diagram of the three beams has no significant difference in the ultimate capacity of the beams. The resistance capacity of the beams were summarized in Table 5-6 as follows.

Table 5-5: Analytical and experimental ultimate capacities of flexure beams

Flexure beams	FEA mid-span UL(kN)	Experimental Mid-Span UL (kN)	FEA & Experimental Mid-Span UL difference (%)	Experimental Mid-Span UL difference form THB-1 (%)
THB-1	72.85	77.01	5.40	-
THB-2	73.78	78.76	6.32	2.27
THB-3	76.09	76.78	0.90	0.3

Where: UL – Ultimate Load

The result in Table 5-5 shows that the use of anchorage or development length further from the support in flexure critical beams have no significant effect on the beam's ultimate capacity.

5.4 Shear Critical Beams Investigation Result

In this investigation, three types of six beams (weak in shear) were studied based on different longitudinal reinforcement end anchorage and development length. Three of them were assessed experimentally and the others were using FEA simulation VecTor2 software, to compare with the experimental result. In all the six specimens, a typical shear failure mechanism was observed. The result and discussion was briefly explained as follows.

5.4.1 Crack Patterns of Shear Critical Beams

5.4.1.1 Experimental Crack patterns of Shear Critical Beams

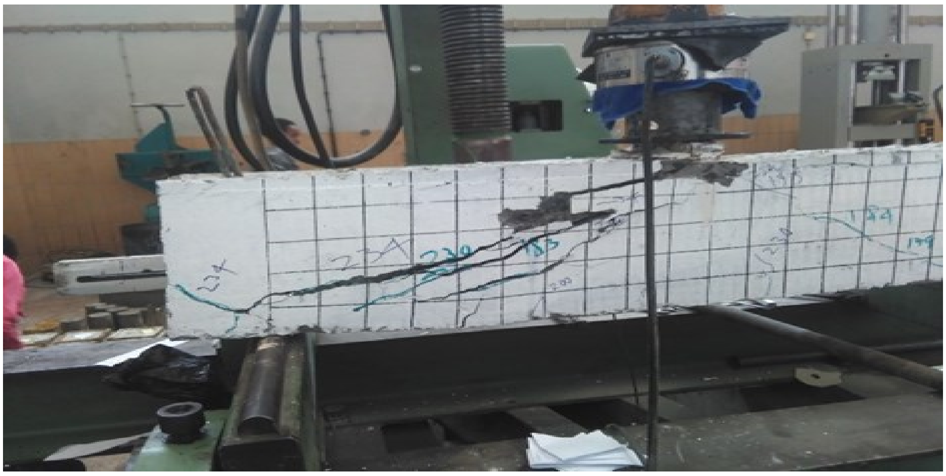

Figure 5-21: Experimental shear failure crack patterns of THB-4

Figure 5-22: Experimental shear failure crack patterns of THB-5

Figure 5-23: Experimental shear failure crack patterns of THB-6

The above figures, (Figure 5-21 to Figure 5-23) show a little bit of crack pattern difference. The crack pattern differences observed in the above figures will be explained in section (5.4.1.3) with the FEA simulation crack pattern results.

5.4.1.2 FEA Crack Patterns of Shear Critical Beams

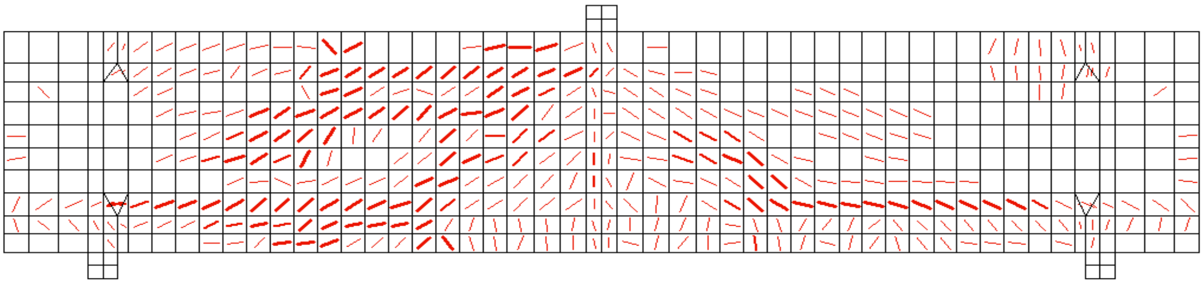

Figure 5-24: FEA shear failure crack patterns of THB-4

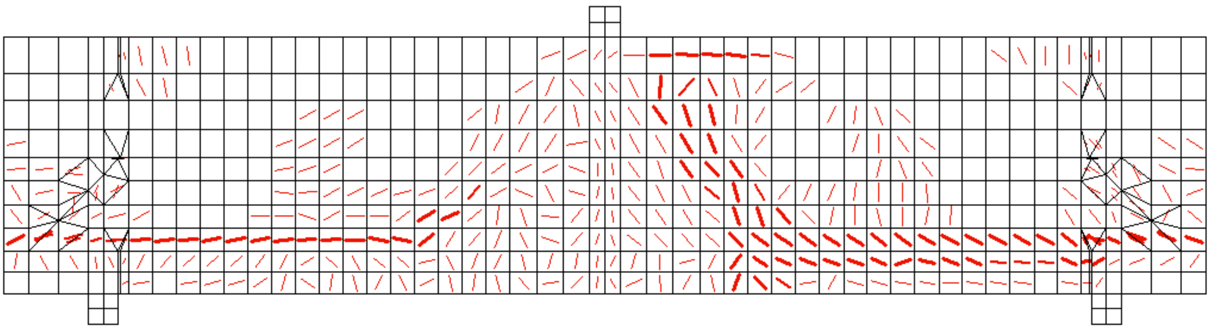

Figure 5-25: FEA shear failure crack patterns of THB-5

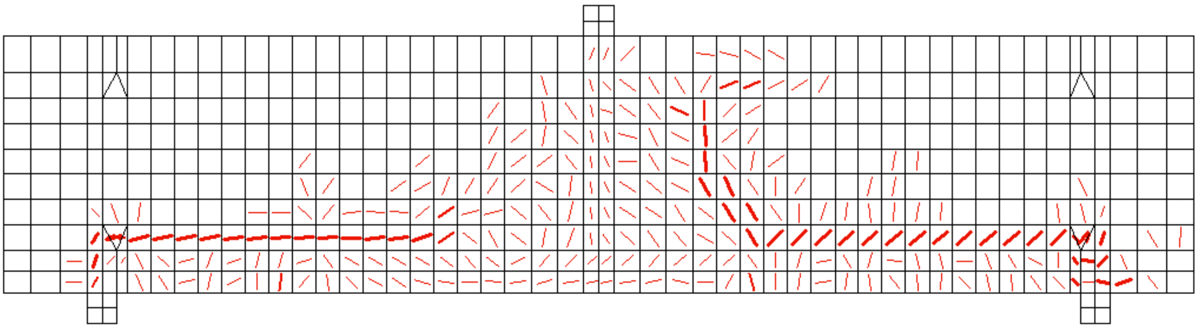

Figure 5-26: FEA shear failure crack patterns of THB-6

As the experimental result, the FEA simulation result shows a little bit of crack patterns difference between THB-4, THB-5, and THB-6.

5.4.1.3 Experimental & FEA Crack Pattern Comparison of Shear Critical Beams

The experimental and FEA crack patterns of shear critical reinforced concrete beams are shown in Figure 5-27 to Figure 5-29.

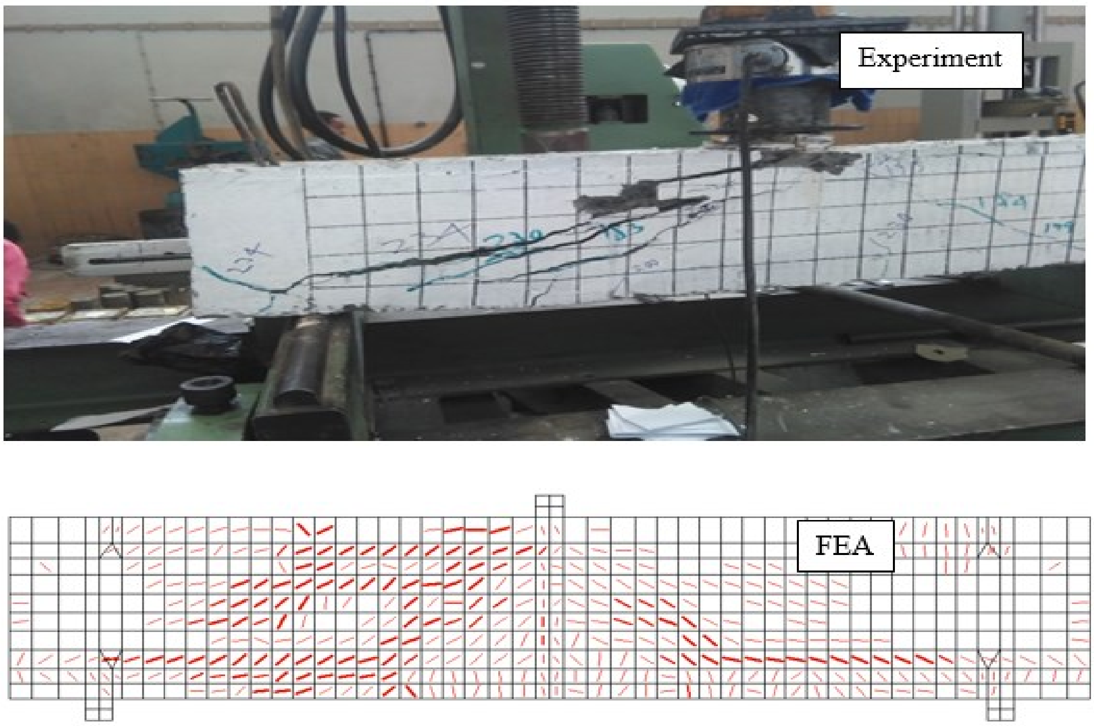

Figure 5-27: Shear failure crack patterns of THB-4

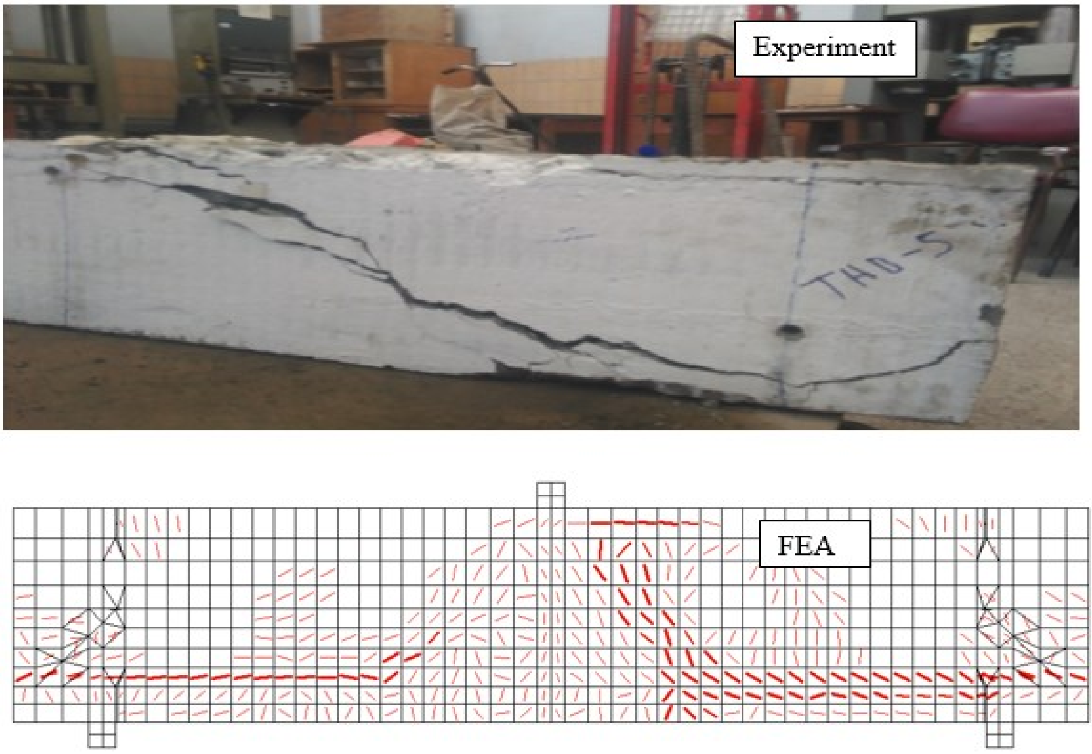

Figure 5-28: Shear failure crack patterns of THB-5

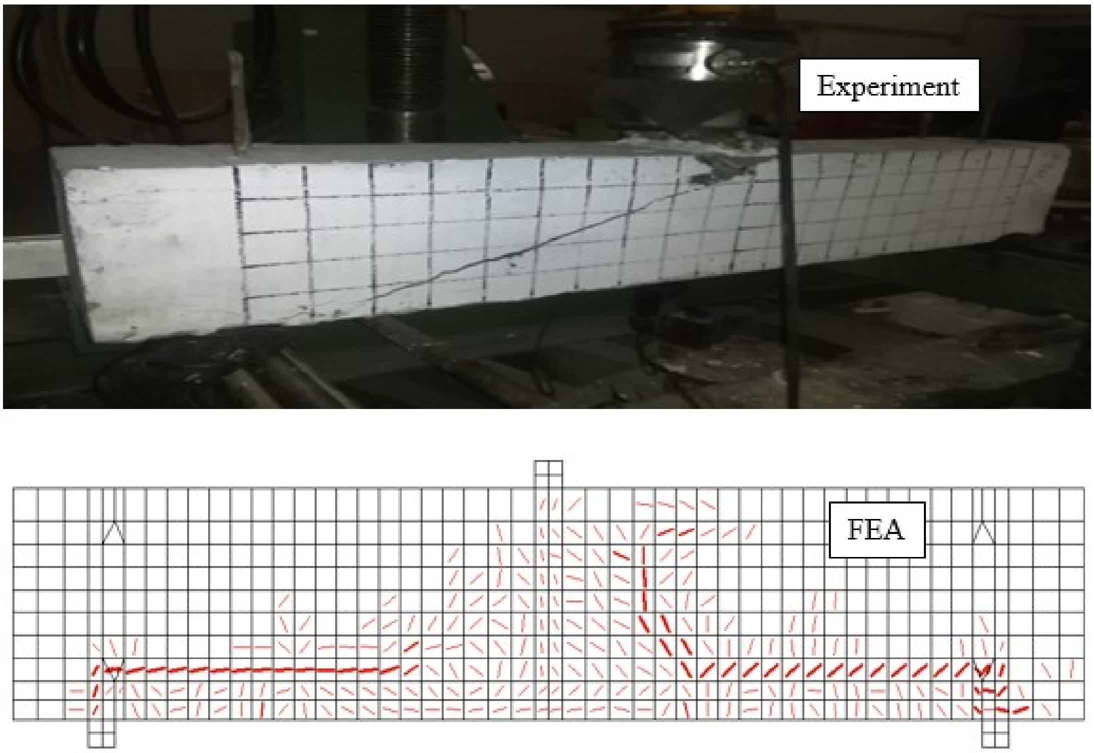

Figure 5-29: Shear failure crack patterns of THB-6

The experimental and the finite element analysis crack pattern results of the three shear critical beams (THB-4, THB-5, and THB-6) were shown in Figure 5-27 – Figure 5-29. The result shows that the experimental and the finite element analysis simulation result gives comparable shear crack patterns for each beam.

5.4.1.4 Comparison of Shear Critical Beams Based on Crack Patterns

In the above figures, (Figure 5-27-5-29), the crack pattern formation difference was observed between shear critical beams (THB-4, THB-5 & THB-6). In THB-4 a typical compression shear failure was observed, where crack patterns were limited within the shear span. The crack patterns observed in THB-5 have been a little bit different from that of THB-4, where the shear failure mechanism seems to anchorage failure and the cracks go further from support to the end face of the beam. Shear crack patterns observed in THB-6 was a significant difference from the other crack patterns observed in THB- 4 & THB-5. The shear crack pattern formation in THB-6 was occurred until the support and not goes farther from the support. As Figure 5-29 shows, the shear crack patterns occurred in the shear span zone and continues to the support but not further continue to the end of the beam face like THB-5.

5.4.2 Shear Critical Beams Load vs Deflection Diagram

5.4.2.1 Experimental Load Vs Deflection Diagram of Shear Critical Beams

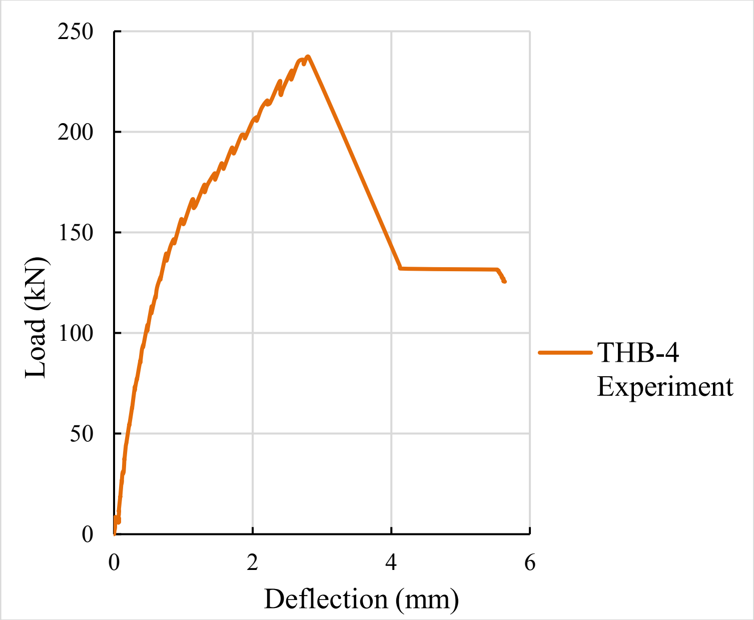

Figure 5-30: Experimental load vs deflection diagram of THB-4

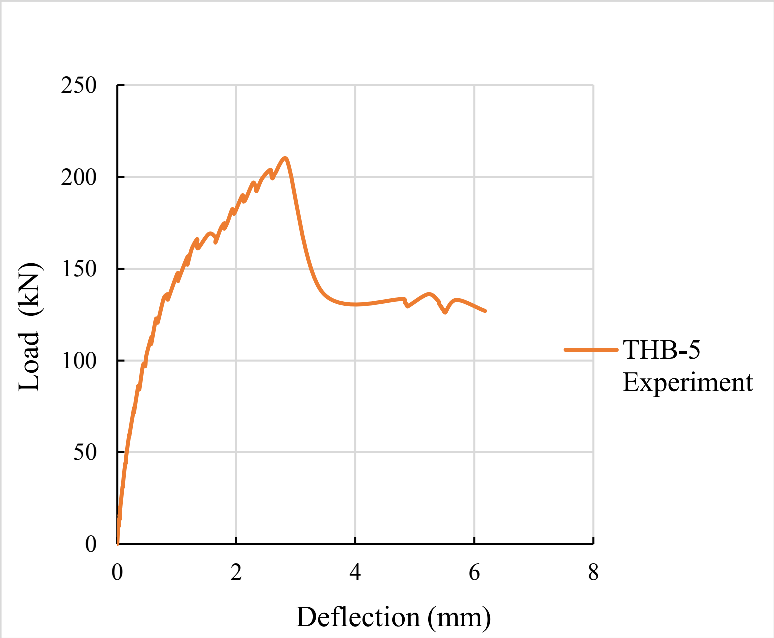

Figure 5-31: Experimental load vs deflection diagram of THB-5

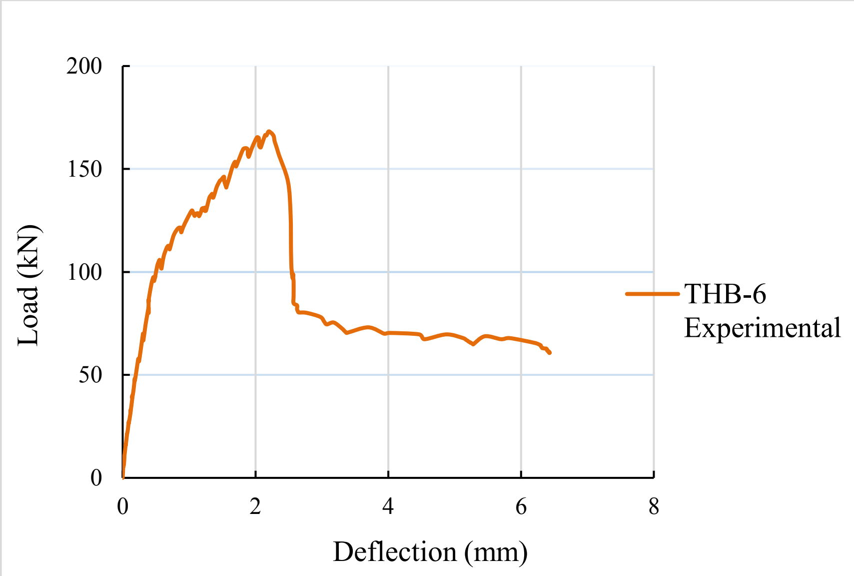

Figure 5-32: Experimental load vs deflection diagram of THB-6

From the experimental load vs deflection diagram shown in Figure 5-30 to Figure 5-32 the ultimate mid-span load of the beams, THB-4, THB-5, and THB-6 are 237.10kN, 209.24kN, and 168.22kN respectively.

5.4.2.2 FEA Load Vs Deflection Diagram of Shear Critical Beams

The finite element analysis load vs deflection diagrams of shear critical beams is shown in Figure 5-33 to Figure 5-35.

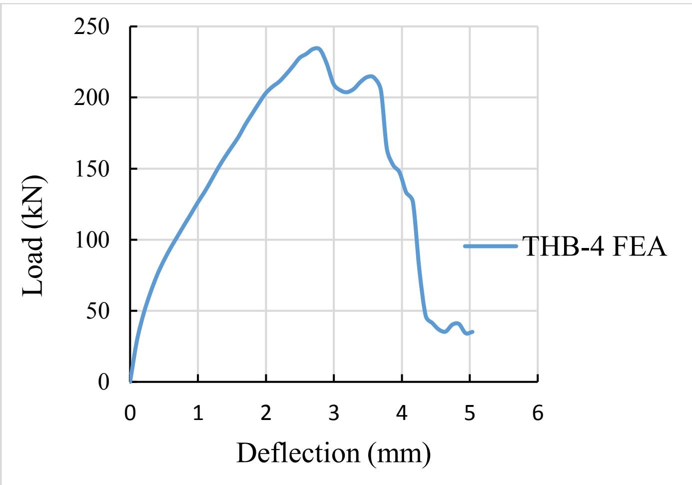

Figure 5-33: FEA load vs deflection diagram THB-4

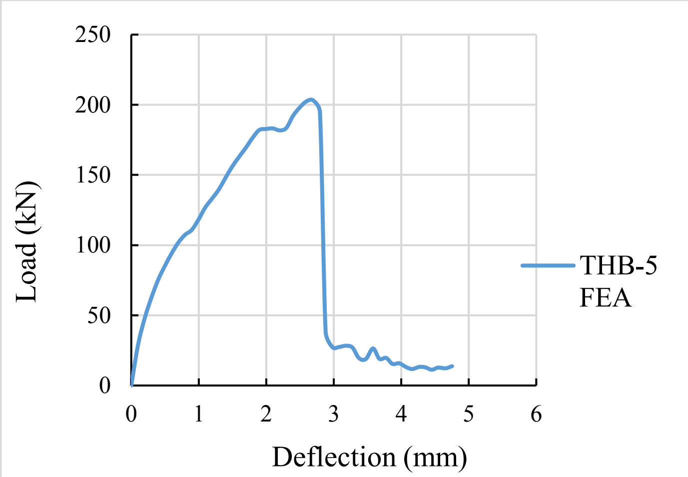

Figure 5-34: FEA load vs deflection diagram THB-5

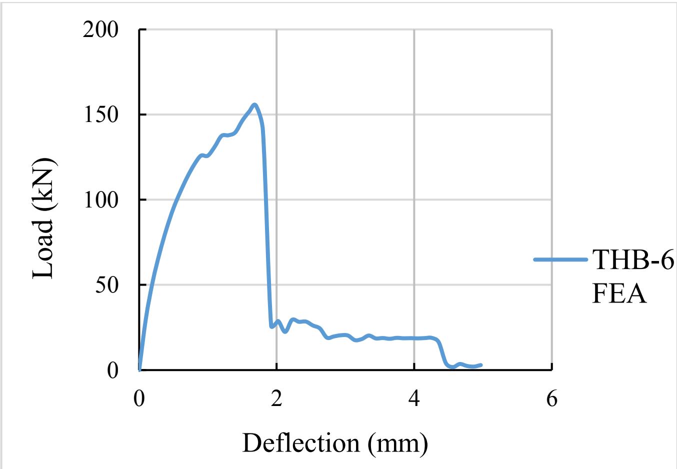

Figure 5-35: FEA load vs deflection diagram THB-6

The finite element analysis ultimate mid-span load of the beams (THB-4, THB-5, and THB-6) are 234.14kN, 203.13kN, and 155.41kN respectively.

5.4.2.3 Experimental & FEA Load vs Deflection Diagram Comparison

The experimental and FEA load vs deflection diagram comparison of shear critical beam's is shown in Figure 5-36 to Figure 5-38.

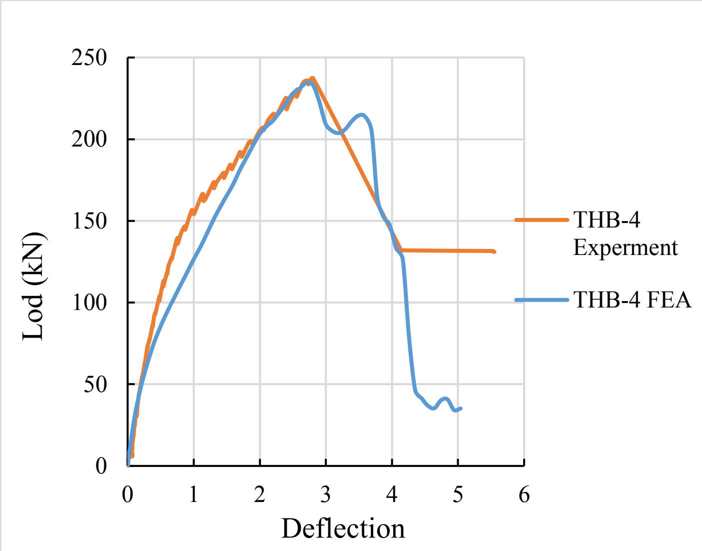

Figure 5-36: Load vs deflection diagram of THB-4

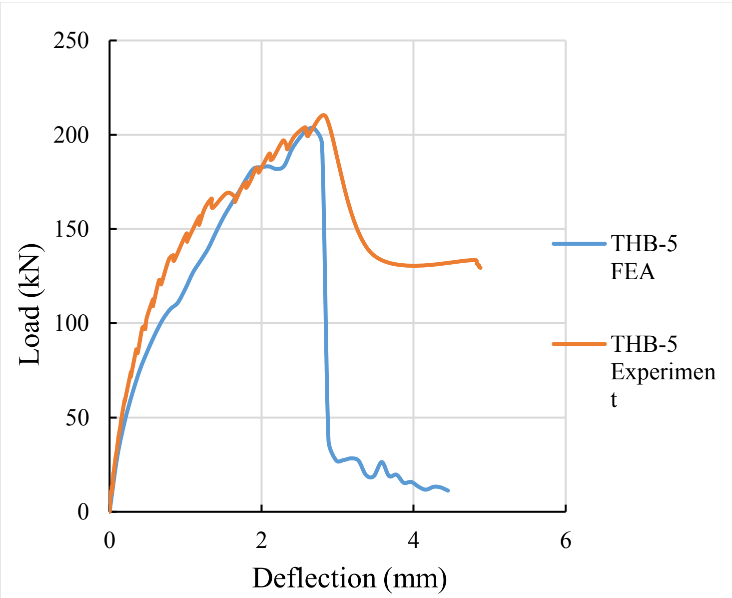

Figure 5-37: Load vs deflection diagram of THB-5

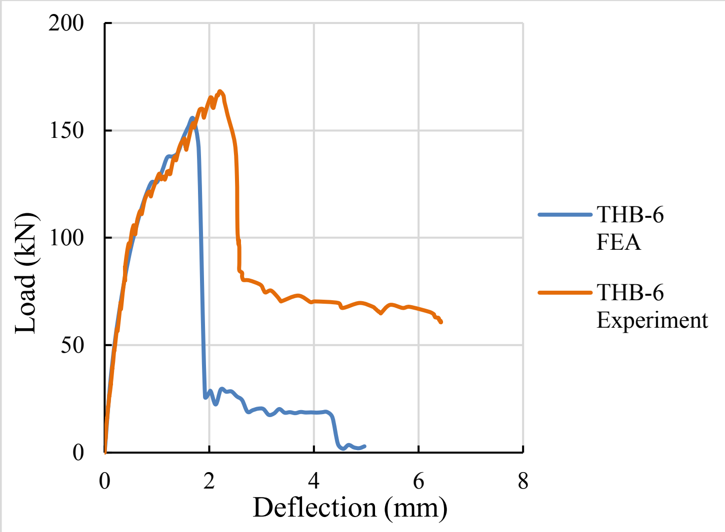

Figure 5-38: Load vs deflection diagram of THB-6

The experimental and FEA load vs deflection diagram of the shear critical beams (THB-4, THB-5, and THB-6) shown in Figure 5-36 to Figure 5-38 have nearly the same load vs deflection diagrams of each beam.

5.4.2.4 Shear Critical Beams Comparison Based on Load Vs Deflection Diagram

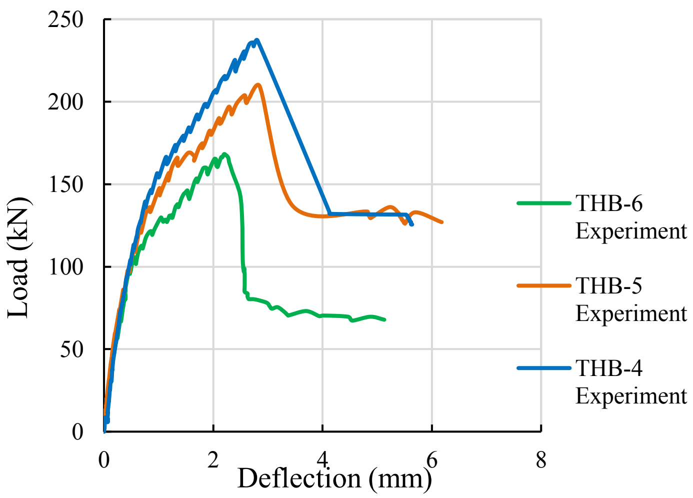

Figure 5-39: Load vs deflection diagram experimental shear critical beams

The load vs deflection diagram of shear critical beams using experimental and finite element analysis simulation are summarized in Figure 5-40.

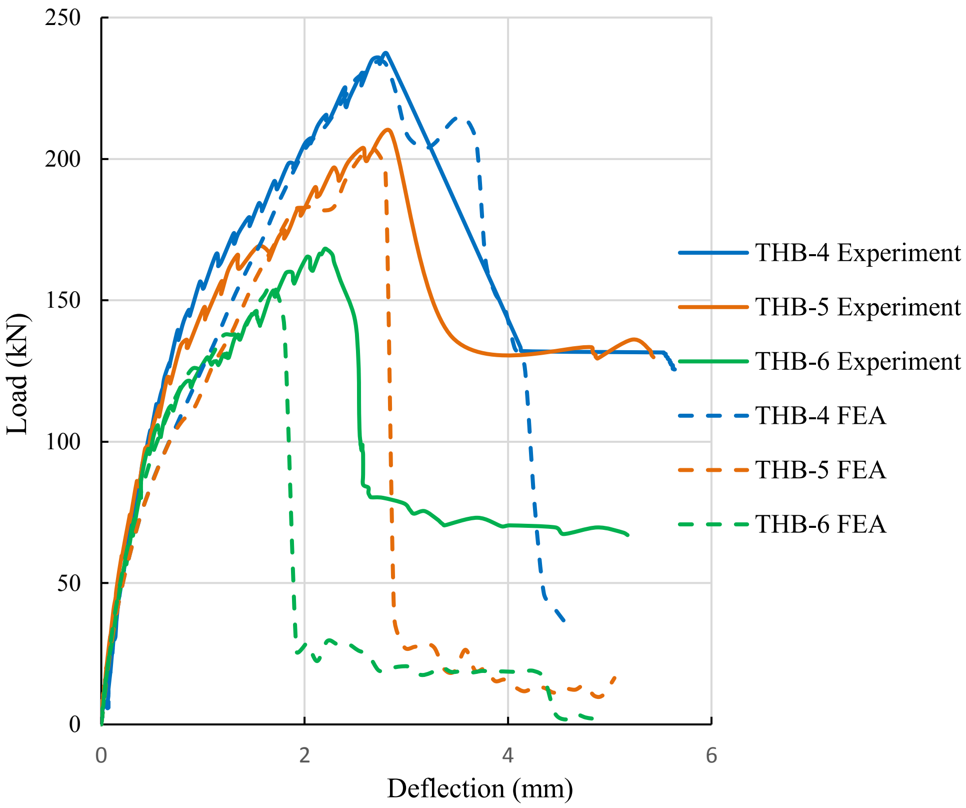

Figure 5-40: Load vs deflection diagram of experimental & FEA shear critical beams

The result in Figure 5-40 shows that the load vs deflection diagram of the three beams have a difference in the ultimate capacity and deflections of the beams. The resistance capacity of the beams was summarized in Table 5-6.

Table 5-6: Experimental and FEA ultimate capacities of shear beams

Shear beams	FEA mid-span UL(kN)	Experimental Mid-Span UL (kN)	FEA & Experimental Mid-Span UL difference (%)	Experimental Mid-Span UL difference formTHB-4 (%)
THB-4	234.14	237.10	1.26	-
THB-5	203.13	209.24	3.01	11.75
THB-6	155.41	168.22	8.24	29.05

Where: UL – Ultimate Load

In general, the use of anchorage or development length further from the support in shear critical beams has a significant effect on beams shear resistance capacity.

CHAPTER 6 CONCLUSION AND RECOMMENDATION

6.1 Conclusion

In this thesis, the effect of longitudinal reinforcement end anchorage on the shear and flexural behavior of reinforced concrete beam has been studied. The investigation was conducted both by experimental investigation and VecTor2 finite element analysis simulation software on three flexure critical and three shear critical beams. Based on the above investigations, the following are concluded.

1. The experimental and finite element analysis simulation results gives comparable result both for flexure critical and shear critical beams.
2. Providing anchorage or development length on longitudinal reinforcement bars further from the support have no significant effect on flexure critical beam's resistance capacity and crack pattern formation.
3. Providing anchorage or development length on longitudinal reinforcement bars further from the support has a significant effect on shear critical beams behavior.
4. Shear critical beam's, longitudinal reinforcement bars that have not developed further from the support lose their ultimate shear capacity by 29.05% than beam's that had longitudinal reinforcement bar development length with 90^o bend or anchorage.
5. Shear critical beam's, longitudinal reinforcement bars that had development length with 135^O bend further from the support lose their ultimate shear capacity by 11.75% than beam's that had longitudinal reinforcement bar development length with 90^O bend or anchorage.
6. In shear critical beam's, providing anchorage or development length on longitudinal reinforcement bars with 135^o bend increases the formation of cracks farther from the support and providing longitudinal reinforcement bars to the support only blocks the formation of cracks farther from the support.

6.2 Recommendation

In this thesis, the effect of longitudinal tensile reinforcement end anchorage and development length from the support on the beam capacity was studied on short beams, where the shear span to depth ratio is 2. The research basically conducted both experimental and software simulation. The effect of tensile reinforcement end anchorage angle and development length on beams capacity needs further study on cylinder (shear span ratio greater than 2.5) and very short or deep beams where the shear span to depth ratio less than 2.

REFERENCES

1. ACI318M-08. (2008). *Building code requirements for structural concrete and commentary.* American Concrete Institute.

2. Ahmet, K. T. (2001). Influence of longitudinal reinforcement type on the shear strength of reinforced concrete beams without transverse reinforcement. *Purdue University*.

3. Amith, S. D., & Balakrishna, B. H. (2015). An experimental study on the Flexural Behavior of Reinforced concrete Beams by partial Replacement of fine aggregate with coal-based Brick Kiln-Ash. *International Research Jornal of Engineering and Technology, Volume: 02 Issue:02*.

4. Arivalagan, S. (2013). Experimental study on the flexural behavior of Reinforced concrete Beams as Reinforcement of Copper slag as fine Aggregate. *Journal of Civil Engineering and Urbanism, Volume 3, Issue 4*, pages 176-182.

5. Bangash, H. M. (1992). *Structural Details in Concrete.* Blackwell Scientific Publications.

6. Chang, H. E. (2009). Shear and Bond Behavior of Reinforced Fly Ash-Based Geopolymer Concrete Beams. *Curtin University of Technology*.

7. Mahdia, & et al. (2015). An experimental study on the flexural strength of reinforced concrete beams with 100% recycled concrete aggregate. *Engineering Structures, Volume 88*, 154-162.

8. Mashhour, & El-Mihilmy, M. (2008). *Design of reinforced Concrete Structure,2nd Edition* (Vol. Volume 1).

9. Moretto, O. (1945). An Investigation of the Strength of Welded Stirrups in Reinforced Concrete Beam. *ACI Material Journal, Vol. 11, no. 42*, pp. 141-162.

10. Mylrea, T. D. (1948). Bond and anchorage. *ACI Jornal, 44(3)*, 521-552.

11. Nawy, E. (2009). *REINFORCED CONCRETE FUNDAMENTAL APPROACH.* New Jersey: Pearson.

12. Pay, A. C., Canbay, E., & Frosch, F. J. (2014). Bond strength of spliced fiber-reinforced polymer reinforcement. *ACI Structural Jornal, 111(2)*, 257-266.

13. Rami, A., & et al. (2014). Behavior of Reinforced concrete beams Strengthened with externally bonded hybrid fiber-reinforced polymer systems. *Material and Design*, 972-982.

14. Rendy, T. (2016). Effect of end anchorage length and stirrup ratio on bond and shear capacity of concrete beams with nonmetallic reinforcement. *Journal of Engineering Science and Technology, 11*, 768-787.

15. Richart. (1927). An Investigation of Web Stresses in Reinforced Concrete Members. *University of Illinois Experiment station*.

16. Sadd, M. (2009). *Elasticity: Theory, Applications, and Numerics, 2nd Edition.* Burlington, Academic Press.

17. Sonal, R., & Sunil, T. (2017). Effect of size and arrangement of tension reinforcement of flexural behavior of reinforced concrete beam. *International Jornal of Current Engineering and Technology, Vol. 7, No. 3*.

18. Standard Ethiopian Building Code. (1995). *Structural Use of Concrete.* Addis Ababa, Ethiopia: Ministry of Works & Urban Development.

19. Wight, K. J., & MacGregor, G. J. (2009). *Reinforced Concrete Mechanics and Design, Six edition.* Scarborough, Ontario: Prentice-Hall, Inc.

20. William, J. K., & Charles, W. T. (1966). Contribution of Longitudinal Steel to Shear Resistance of Reinforced Concrete Beams. *ACI Material Journal*, 325-344.

21. Wong, P. S., & Vecchoio, F. J. (2002). *VecTor2 and Formworks Use's Manual.* University of Toronto, Canada.

APPENDIX A

The procedures of concrete mix design used in the preparation of beam test specimens were presented as follows.

1. Choice of slump

Table A-1 Recommended slumps for various types of construction (ACI-2111_91)

Types of construction	Maximum Slump (mm)	Minimum Slump (mm)
Reinforced foundation walls & footings	75	25
Plain footings and substructure walls	75	25
Beams and reinforced walls	100	25
Building columns	100	25
Pavements and slabs	75	25
Mass concrete	75	25

From the table above, for reinforced concrete beam the recommended maximum and minimum slumps are 100mm and 25mm respectively.

2. Maximum size of aggregates
   - Fine aggregates =4.75mm
   - Coarse aggregates =20mm
3. Estimation of mixing water and air content

The mix is none air-entrained mix design. From the ACI standard for slump value 75-100 and maximum size of aggregate 20mm, the water content in 1m^3 concrete is 203kg/m^3.

4. Water to cement ratio estimation

From ACI-2111_91 the compressive strength of 30Mpa concrete, the recommended w/c ratio is 0.61 (for non-air entrained concrete mix).

5. Cement content estimation

For slump value 75mm-100mm the water content is 203kg/m^3.

Cement content = water content divided by w/c

= 203/0.61= 332.79kg/m^3

6. Coarse aggregate content estimation

From ACI, for 20mm maximum size of coarse aggregate and 2.49 fines modules of sand, the volume of coarse aggregate in 1m^3 concrete is 0.652m^3.

Mass of coarse aggregate = 0.62*1687

= 1100.05kg/m^3

7. Fine aggregate content estimation

The mass of fine aggregate needed for 1m^3 of concrete is estimated as follows using the weight method of batching. The unit weight of concrete from ACI for a maximum size of coarse aggregate (20mm) is 2350.83kg/m^3.

Fine aggregate content = 2350.83-332.79-1100.05

= 714.99kg/m^3

8. Moisture adjustment

The difference between moisture content and absorption capacity of aggregates are as shown below.

Fine aggregate: 3.3% - 1.4% = 1.9%, moisture will be deducted

Coarse aggregate: 1.97% -0.44% = 1.53%, moisture will be deducted

Net water required = 203 – 714.99*0.019 – 1100.05*0.015

= 172.91kg/m^3

9. Final composition

The composition of the constituent materials is summarized in Table A.

Table A-2: Plain concrete mix proportion

Materials	Weight (kg/m^3)	Ratio
Cement	332.79	1
Fine aggregate	714.99	2.15
Coarse aggregate	1100.05	3.31
Water	172.91	0.52
Unit wet of concrete	2350.88	

APPENDIX B

THB-1 experimental load vs deflection result in tabular form.

Deflection (mm)	Load (kN)	Deflection (mm)	Load (kN)	Deflection (mm)	Load (kN)	Deflection (mm)	Load (kN)
0.00	0.00	2.06	46.27	9.68	69.78	22.16	73.53
0.00	0.25	2.06	46.02	9.68	69.53	22.17	70.53
0.02	0.50	2.06	45.77	9.68	69.53	22.54	73.78
0.06	2.50	2.06	45.52	10.14	74.03	22.57	70.53
0.08	3.75	2.27	51.27	10.22	71.53	22.82	73.28
0.08	3.50	2.30	49.77	10.34	73.28	22.97	70.53
0.08	3.50	2.30	49.27	10.85	72.53	23.16	73.03
0.15	7.50	2.30	49.02	10.87	71.53	23.37	70.78
0.18	8.25	2.30	48.77	11.38	74.28	23.38	71.28
0.18	8.25	2.30	48.77	11.42	70.53	23.76	71.28
0.18	8.00	2.51	54.27	11.63	73.53	23.78	70.03
0.28	13.01	2.52	53.02	11.87	71.53	23.78	69.53
0.31	13.51	2.52	52.52	11.89	71.28	24.26	73.53
0.31	13.26	2.52	52.27	12.35	72.78	24.28	70.53
0.32	14.51	2.64	56.02	12.36	72.03	24.29	69.53
0.41	18.01	2.74	57.27	12.80	74.53	24.30	69.28
0.46	19.51	2.75	56.77	12.82	72.53	24.30	69.03
0.47	19.26	2.76	56.52	13.06	75.28	24.30	68.78
0.47	19.01	2.76	56.02	13.25	72.78	24.31	68.53
0.57	22.76	2.76	56.02	13.55	75.78	24.31	68.28
0.63	24.26	2.88	59.02	13.67	73.28	24.31	68.28
0.66	24.76	3.05	60.77	13.83	75.03	24.31	68.03
0.66	24.26	3.09	60.02	14.15	73.78	24.32	68.03
0.66	24.26	3.09	59.27	14.17	72.78	24.32	67.78
0.68	25.26	3.09	59.02	14.62	74.53	24.32	67.78
0.73	27.01	3.09	58.77	14.63	73.03	24.32	67.53
0.81	29.26	3.09	58.77	14.63	72.53	24.33	67.53
0.85	29.51	3.18	61.27	14.89	74.53	24.33	67.28
0.84	29.01	3.26	62.78	14.96	74.03	24.33	67.28
0.88	30.51	3.54	60.27	14.97	73.03	24.33	67.28
1.01	33.01	3.55	59.52	15.30	76.28	24.33	67.28
1.09	32.51	3.55	59.27	15.33	73.53	24.33	67.03
1.10	31.51	3.91	62.27	15.52	76.03	24.33	67.03
1.10	31.26	4.02	61.27	15.76	74.03	24.33	67.03
1.20	34.26	4.02	60.77	15.82	74.03	24.33	67.03
1.30	36.26	4.26	63.53	16.18	74.53	24.33	66.78
1.32	35.76	4.39	63.28	16.19	73.78	24.33	66.78

1.32	35.51	4.44	62.78	16.55	76.03	24.33	66.78
1.32	35.26	4.44	62.27	16.59	74.03	24.33	66.78
1.32	35.01	4.69	65.53	16.60	73.53	24.33	66.78
1.32	34.76	4.83	63.78	17.01	76.53	24.33	66.53
1.32	34.76	4.83	63.28	17.03	74.03	24.33	66.53
1.32	34.76	5.00	66.03	17.22	76.53	24.33	66.53
1.32	34.76	5.21	65.78	17.47	74.28	24.33	66.53
1.32	34.51	5.21	64.78	17.50	73.53	24.33	66.53
1.32	34.51	5.50	67.78	18.02	74.78	24.33	66.28
1.32	34.51	5.53	66.03	18.03	73.53	24.33	66.28
1.32	34.51	5.63	67.53	18.45	76.28	24.33	66.28
1.33	34.26	5.92	67.53	18.51	74.03	24.33	66.28
1.33	34.26	5.92	66.78	18.52	73.28	24.33	66.28
1.33	34.26	6.31	69.78	18.52	72.78	24.33	66.28
1.33	34.26	6.33	68.03	18.57	73.53	24.33	66.28
1.33	34.26	6.33	67.53	18.82	74.28	24.33	66.28
1.33	34.01	6.79	70.28	18.83	73.53	24.33	66.03
1.33	34.01	6.81	68.53	19.15	74.53	24.33	66.03
1.33	34.01	6.89	69.53	19.16	73.53	24.33	66.03
1.33	34.01	7.45	69.03	19.39	76.03	24.34	66.03
1.33	34.26	7.46	68.28	19.42	73.78	24.34	66.03
1.51	40.02	7.73	71.28	19.43	73.03	24.33	66.03
1.55	40.27	8.02	69.53	19.84	76.53	24.34	66.03
1.56	39.77	8.03	68.78	19.94	73.53	24.33	66.03
1.70	43.52	8.42	72.28	19.95	72.53	24.34	65.78
1.79	44.52	8.56	70.03	20.37	75.78	24.34	65.78
1.79	43.52	8.58	69.28	20.41	73.28	24.34	65.78
1.79	43.02	9.09	71.03	20.42	72.28	24.34	65.78
1.79	43.02	9.11	70.03	20.45	72.53	24.34	65.78
1.79	42.77	9.15	70.53	20.87	73.53	24.34	65.78
1.79	42.52	9.53	72.78	20.90	72.28	24.34	65.78
1.79	42.52	9.65	71.03	21.28	73.28	24.34	65.78
1.79	42.27	9.67	70.53	21.28	71.53	24.34	65.78
1.92	46.27	9.67	70.28	21.75	72.78	24.34	65.78
2.05	46.77	9.67	70.03	21.76	70.53	24.34	65.53

THB-2 experimental load vs deflection result in tabular form.

Deflection (mm)	Load (kN)	Deflection (mm)	Load (kN)	Deflection (mm)	Load (kN)	Deflection (mm)	Load (kN)
0.00	0.00	2.32	54.27	9.92	70.93	21.78	73.59
0.02	1.00	2.32	54.27	9.93	71.59	21.78	74.01
0.03	1.00	2.32	54.27	9.93	70.68	21.78	74.18
0.06	2.00	2.32	54.02	9.93	71.43	21.78	73.18
0.06	2.00	2.32	54.02	9.93	71.26	21.78	73.43
0.06	1.75	2.32	54.02	9.93	70.76	21.78	74.01
0.13	3.75	2.32	54.02	9.93	71.51	21.78	73.93
0.13	3.75	2.32	54.02	9.93	71.76	21.79	72.59
0.13	3.50	2.32	53.77	9.93	70.93	21.79	73.43
0.13	3.50	2.32	53.77	9.93	71.68	21.79	73.09
0.13	3.50	2.32	53.77	9.93	71.09	21.79	72.34
0.13	3.50	2.32	53.77	9.93	70.76	21.79	73.01
0.13	3.50	2.32	53.77	9.93	71.43	21.79	72.76
0.13	3.50	2.32	53.77	9.93	70.84	21.79	73.34
0.13	3.50	2.32	53.52	9.94	70.59	21.79	72.68
0.13	3.50	2.32	53.52	10.68	75.34	21.79	72.93
0.13	3.25	2.54	60.77	10.69	73.26	21.79	72.51
0.13	3.25	2.81	62.02	10.70	73.51	21.79	72.26
0.13	3.25	2.81	61.02	11.49	75.59	21.79	72.93
0.12	3.50	2.82	60.77	11.51	74.26	21.79	71.68
0.12	3.25	2.83	60.77	11.89	76.68	21.79	73.34
0.12	3.25	3.44	61.65	12.27	75.09	21.79	71.76
0.33	8.50	3.44	61.89	12.28	75.59	21.79	72.59
0.52	13.26	3.44	63.78	12.98	77.59	21.79	71.93
0.52	13.01	3.44	63.53	13.12	74.09	21.79	72.43
0.58	14.51	3.44	63.28	13.12	74.09	21.79	72.59
0.91	23.51	3.44	63.28	13.36	75.93	21.79	71.93
0.95	24.01	3.44	63.03	13.97	76.34	21.79	72.68
0.95	23.76	3.44	63.03	13.98	75.26	21.79	71.59
1.02	25.76	3.44	62.78	14.89	78.43	21.79	71.18
1.38	35.76	3.44	62.78	15.04	76.26	21.79	73.51
1.38	35.26	3.44	62.78	15.10	77.43	21.79	71.68
1.38	35.01	3.80	63.32	16.37	73.84	21.79	71.76

1.41	36.51	4.06	63.35	16.39	73.84	21.79	71.34
1.83	47.77	4.06	63.35	16.40	74.43	21.79	71.01
1.83	47.02	4.21	64.12	16.40	73.34	21.79	71.18
1.83	46.77	4.71	64.12	16.81	75.26	21.79	71.51
1.83	46.52	4.71	63.98	17.29	75.59	21.79	70.84
1.83	46.27	4.71	63.98	17.31	74.59	21.79	71.43
1.83	46.27	4.71	63.98	18.12	77.68	21.79	70.93
1.83	46.02	4.71	65.26	18.20	76.34	21.79	70.93
2.30	57.77	5.29	68.26	18.21	75.59	21.79	71.34
2.32	57.02	5.38	68.59	19.03	78.76	21.79	70.51
2.32	56.52	5.38	67.93	19.05	76.84	21.79	70.76
2.32	56.27	5.39	67.42	19.07	78.59	21.79	70.01
2.32	56.02	5.98	70.34	19.90	78.18	21.79	69.68
2.32	55.77	6.07	68.76	19.92	77.43	21.79	69.51
2.32	55.77	6.07	68.34	19.98	77.68	21.79	69.01
2.32	55.52	6.07	69.09	21.12	74.01	21.79	69.51
2.32	55.52	6.87	69.01	21.14	75.09	21.79	68.76
2.32	55.52	6.87	67.84	21.15	73.76	21.79	69.01
2.32	55.27	6.87	68.51	21.15	74.43	21.79	68.84
2.32	55.27	6.88	68.76	21.16	74.43	21.79	68.76
2.32	55.02	7.27	70.93	21.59	75.09	21.79	68.43
2.32	55.02	7.55	70.59	21.76	75.51	21.79	68.59
2.32	55.02	7.56	70.09	21.77	74.18	21.79	68.84
2.32	54.77	8.15	73.93	21.77	74.26	21.79	68.43
2.32	54.77	8.25	72.18	21.77	74.09	21.79	69.01
2.32	54.77	8.27	71.51	21.78	74.51	21.79	68.18
2.32	54.77	8.28	73.18	21.78	74.68	21.79	68.84
2.32	54.52	8.28	71.84	21.78	74.01	21.79	68.01
2.32	54.52	8.90	74.01	21.78	73.51	21.79	67.84
2.32	54.52	9.02	73.51	21.78	73.09	21.79	67.76
2.32	54.52	9.03	72.68	21.78	73.68	21.79	67.51
2.32	54.52	9.87	71.59	21.78	73.59	21.79	67.51
2.32	54.52	9.91	71.34	21.78	74.09	21.79	67.43

THB-3 experimental load vs deflection result in tabular form.

Deflection (mm)	Load (kN)	Deflection (mm)	Load (kN)	Deflection (mm)	Load (kN)	Deflection (mm)	Load (kN)
0.00	0.00	2.50	51.77	8.39	72.28	18.35	71.53
0.06	2.75	2.51	52.02	8.59	70.78	18.36	70.78
0.06	2.50	2.52	52.02	8.59	70.03	18.48	72.78
0.06	2.50	2.60	54.02	8.90	73.03	18.60	71.28
0.15	6.75	2.60	53.27	8.96	70.53	18.63	71.03
0.15	6.50	2.60	52.77	8.97	70.03	18.86	71.78
0.17	7.50	2.77	57.27	9.29	71.78	18.88	70.78
0.25	11.00	2.82	57.02	9.30	70.53	19.22	73.53
0.26	10.75	2.82	56.02	9.35	71.03	19.26	71.28
0.25	10.75	2.82	55.77	9.59	71.28	19.43	73.53
0.32	14.01	2.95	59.27	9.59	70.53	19.58	71.53
0.35	14.76	2.94	58.02	9.82	73.53	19.60	70.78
0.35	14.51	2.94	57.52	9.93	71.53	19.84	73.78
0.45	18.76	3.03	60.02	9.94	70.78	19.91	71.28
0.46	18.26	3.17	62.53	10.23	73.53	20.01	72.53
0.50	20.01	3.22	61.78	10.27	71.53	20.23	71.53
0.65	23.01	3.22	61.02	10.28	71.03	20.25	70.78
0.65	22.51	3.23	61.28	10.54	72.78	20.58	71.53
0.73	25.26	3.57	63.53	10.55	71.53	20.72	73.03
0.87	27.26	3.60	62.03	10.60	72.28	20.94	71.28
0.87	26.76	3.60	61.53	10.82	72.53	21.38	73.03
0.89	27.26	3.60	61.02	10.83	71.53	21.47	71.78
1.07	31.26	3.60	60.77	11.08	74.78	21.80	71.78
1.08	30.26	3.60	60.77	11.18	72.78	22.02	73.28
1.11	30.51	3.60	60.52	11.19	72.03	22.20	70.78
1.30	35.26	3.70	63.28	11.43	74.53	22.51	71.78
1.30	34.01	3.94	64.03	11.47	72.78	22.62	69.53
1.31	33.76	3.95	62.53	11.63	74.78	22.95	69.03
1.51	38.52	3.96	62.28	11.86	73.53	23.12	68.53
1.55	38.27	4.15	64.53	11.87	72.78	23.35	67.03
1.55	37.77	4.32	62.78	12.23	75.03	23.70	68.53
1.55	37.52	4.33	62.28	12.25	73.53	23.76	66.53
1.55	37.27	4.33	62.03	12.53	76.78	24.15	67.28
1.55	37.02	4.61	64.28	12.58	74.03	24.22	66.78
1.55	37.02	4.62	63.28	12.59	73.28	24.52	66.53
1.55	36.77	4.62	63.03	12.96	73.53	24.56	65.78

1.55	36.77	4.81	65.53	12.97	72.78	24.85	66.28
1.55	36.52	4.94	64.78	13.26	75.03	24.96	67.03
1.55	36.52	4.95	64.03	13.28	73.28	25.26	66.03
1.68	40.77	4.96	63.78	13.58	76.28	25.50	67.78
1.79	42.52	4.96	63.53	13.63	73.28	25.55	65.53
1.79	41.77	4.96	63.28	13.68	73.28	26.05	67.53
1.79	41.27	4.96	63.28	13.98	73.03	26.10	65.03
1.79	41.02	5.25	66.78	14.00	72.03	26.12	64.53
1.79	40.77	5.34	65.28	14.26	73.28	26.12	64.28
1.79	40.52	5.34	64.78	14.28	71.78	26.13	63.78
1.79	40.52	5.47	67.28	14.46	74.53	26.13	63.78
1.79	40.27	5.67	67.28	14.55	72.28	26.14	63.53
1.79	40.27	5.70	66.28	14.62	72.78	26.14	63.28
1.79	40.02	5.71	66.03	14.90	72.03	26.14	63.28
1.79	39.77	5.88	69.03	14.91	71.53	26.14	63.03
1.79	39.77	6.02	67.28	15.28	72.78	26.14	63.03
2.01	46.27	6.02	66.78	15.30	71.78	26.15	62.78
2.02	45.02	6.23	70.03	15.61	74.03	26.15	62.78
2.02	44.52	6.39	68.03	15.64	71.78	26.15	62.78
2.02	44.27	6.39	67.53	15.80	74.03	26.16	62.53
2.02	44.02	6.60	70.28	15.98	72.03	26.16	62.53
2.02	43.77	6.70	69.03	15.99	71.28	26.17	62.53
2.02	43.77	6.71	68.28	16.31	72.78	26.20	62.53
2.04	44.52	6.81	70.28	16.34	71.28	26.20	62.53
2.19	48.52	7.04	70.03	16.55	74.03	26.20	62.28
2.23	48.27	7.06	69.03	16.63	71.03	26.20	62.28
2.23	47.77	7.06	68.53	16.64	70.53	26.20	62.28
2.23	47.27	7.38	71.78	16.96	72.03	26.20	62.28
2.35	50.77	7.44	69.78	16.98	70.78	26.20	62.28
2.44	52.02	7.46	69.28	17.29	72.53	26.20	62.03
2.44	50.77	7.83	71.28	17.30	70.78	26.20	62.03
2.44	50.52	7.85	69.78	17.59	73.78	26.20	62.03
2.44	50.02	7.85	69.28	17.65	71.03	26.20	62.03
2.44	49.77	8.06	72.03	17.96	73.53	26.20	62.03
2.43	49.77	8.23	70.53	18.01	71.03	26.20	61.78
2.44	49.77	8.24	69.78	18.12	72.53	26.20	61.78

THB-4 experimental load vs deflection result in tabular form.

Deflection (mm)	Load (kN)	Deflection (mm)	Load (kN)	Deflection (mm)	Load (kN)	Deflection (mm)	Load (kN)
0.00	0.00	0.06	6.75	1.18	163.57	5.60	127.80
0.01	2.75	0.07	6.50	1.30	173.57	5.60	127.80
0.01	2.50	0.06	6.50	1.30	171.07	5.60	127.80
0.01	3.75	0.06	8.25	1.31	170.07	5.60	127.80
0.01	3.50	0.06	7.75	1.35	173.82	5.60	127.55
0.01	3.25	0.07	10.00	1.45	179.32	5.60	127.55
0.01	4.75	0.07	11.76	1.46	177.32	5.60	127.55
0.01	4.00	0.07	11.76	1.46	176.32	5.60	127.55
0.01	4.00	0.07	11.51	1.55	184.32	5.60	127.55
0.01	5.50	0.07	11.51	1.57	183.57	5.60	127.30
0.01	4.50	0.07	11.51	1.58	182.07	5.61	127.30
0.01	5.00	0.07	11.26	1.58	181.57	5.61	127.30
0.01	5.50	0.07	11.26	1.70	192.08	5.61	127.30
0.01	5.25	0.07	11.26	1.72	190.58	5.61	127.05
0.02	6.25	0.07	12.26	1.73	189.33	5.61	127.05
0.02	5.75	0.09	18.76	1.84	198.33	5.61	127.05
0.02	5.75	0.09	18.51	1.89	198.33	5.61	127.05
0.02	6.50	0.11	26.76	1.89	196.83	5.62	127.05
0.02	6.00	0.11	25.26	2.00	205.33	5.62	127.05
0.02	6.00	0.12	30.01	2.06	207.33	5.62	126.80
0.02	7.00	0.13	31.26	2.06	205.58	5.62	126.80
0.02	6.50	0.13	30.51	2.13	211.84	5.62	126.80
0.02	7.00	0.13	30.01	2.21	215.59	5.62	126.80
0.02	7.25	0.14	31.26	2.21	213.59	5.62	126.80
0.02	6.75	0.15	37.77	2.25	214.34	5.62	126.80
0.02	7.75	0.15	37.02	2.39	225.09	5.62	126.80
0.02	7.25	0.17	44.02	2.39	221.84	5.62	126.55
0.02	7.00	0.18	45.52	2.40	220.34	5.62	126.55
0.02	8.00	0.18	45.77	2.40	219.59	5.62	126.55
0.02	7.50	0.22	54.77	2.40	218.84	5.62	126.55
0.02	8.50	0.22	54.02	2.41	218.34	5.62	126.55
0.02	7.75	0.26	63.03	2.44	221.59	5.62	126.30
0.02	7.75	0.26	63.03	2.56	230.34	5.62	126.55
0.02	7.75	0.26	62.53	2.56	227.34	5.62	126.55
0.02	7.75	0.30	73.28	2.56	226.09	5.62	126.30
0.02	8.50	0.30	71.53	2.66	234.84	5.62	126.30

0.02	7.75	0.30	72.03	2.73	235.85	5.62	126.30
0.02	7.75	0.33	77.53	2.74	233.59	5.62	126.30
0.02	7.75	0.33	76.78	2.81	237.10	5.62	126.30
0.02	7.75	0.34	78.78	4.12	133.55	5.62	126.30
0.02	7.75	0.38	86.54	4.13	132.05	5.62	126.30
0.02	7.75	0.38	85.29	5.53	131.55	5.62	126.30
0.02	8.25	0.40	91.29	5.53	131.30	5.62	126.30
0.02	7.75	0.42	94.04	5.54	131.05	5.62	126.05
0.02	7.75	0.42	93.04	5.55	131.05	5.62	126.05
0.02	7.50	0.48	103.79	5.55	130.80	5.62	126.05
0.02	7.50	0.48	101.04	5.55	130.55	5.62	126.05
0.02	7.50	0.48	101.04	5.55	130.55	5.62	126.05
0.02	7.50	0.54	113.05	5.55	130.55	5.62	126.05
0.02	7.50	0.54	110.55	5.55	130.30	5.62	126.05
0.02	7.50	0.54	109.79	5.55	130.30	5.62	126.05
0.02	7.25	0.58	116.05	5.56	130.05	5.62	126.05
0.07	7.25	0.60	118.55	5.56	130.05	5.62	125.80
0.07	7.25	0.60	117.55	5.56	130.05	5.62	125.80
0.07	7.25	0.62	122.55	5.57	129.80	5.62	125.80
0.06	7.25	0.67	127.80	5.57	129.80	5.63	125.80
0.07	8.00	0.67	126.55	5.57	129.55	5.62	125.80
0.07	7.25	0.67	126.80	5.57	129.30	5.63	125.80
0.07	8.00	0.75	139.31	5.57	129.30	5.63	125.80
0.06	7.00	0.76	137.06	5.58	129.05	5.63	125.80
0.06	7.00	0.76	136.06	5.58	129.05	5.63	125.80
0.06	6.75	0.81	142.56	5.59	128.80	5.63	125.80
0.07	6.75	0.86	146.56	5.59	128.80	5.63	125.80
0.06	7.25	0.87	145.31	5.59	128.55	5.63	125.80
0.06	6.50	0.87	144.56	5.59	128.55	5.63	125.80
0.06	7.00	0.97	156.56	5.59	128.55	5.63	125.55
0.06	6.25	0.99	155.56	5.59	128.30	5.63	125.55
0.06	6.75	1.00	154.06	5.59	128.30	5.63	125.55
0.07	6.00	1.01	154.56	5.59	128.05	5.63	125.55
0.06	6.50	1.13	166.32	5.59	128.05	5.63	125.55
0.07	6.00	1.15	163.32	5.60	128.05	5.63	125.55
0.06	5.75	1.15	162.07	5.60	128.05	5.63	125.55

THB-5 experimental load vs deflection result in tabular form.

Deflection (mm)	Load (kN)	Deflection (mm)	Load (kN)	Deflection (mm)	Load (kN)
0.00	0.00	0.49	102.96	5.41	130.75
0.01	7.34	0.57	112.52	5.43	129.86
0.01	8.45	0.57	110.07	5.45	128.97
0.01	8.22	0.57	108.96	5.45	128.53
0.01	8.22	0.65	122.74	5.47	128.08
0.01	8.22	0.68	122.52	5.47	127.64
0.01	8.00	0.68	120.74	5.48	127.42
0.02	9.56	0.78	133.86	5.49	127.19
0.02	9.78	0.84	136.09	5.49	126.75
0.02	9.56	0.84	133.20	5.49	126.53
0.02	10.67	0.85	133.20	5.50	126.31
0.02	10.00	1.01	147.43	5.51	126.08
0.02	10.00	1.02	144.53	5.51	126.08
0.02	11.11	1.02	143.20	5.70	132.97
0.03	10.67	1.03	144.31	6.18	126.97
0.03	10.45	1.18	156.54	6.22	125.19
0.03	11.34	1.18	153.43	6.36	128.97
0.03	11.56	1.18	152.32	6.87	126.31
0.03	11.11	1.25	160.77	6.91	124.53
0.03	12.45	1.34	166.10	7.09	128.75
0.03	12.00	1.34	163.21	7.68	122.74
0.03	11.78	1.36	161.21	7.72	120.74
0.03	13.35	1.54	169.00	7.76	119.63
0.03	12.67	1.65	166.99	8.21	118.52
0.03	13.57	1.65	165.21	8.26	116.52
0.04	14.01	1.65	164.32	8.28	115.63
0.04	13.35	1.74	172.11	8.93	116.74
0.04	14.46	1.80	174.78	9.05	112.96
0.04	14.46	1.80	172.78	9.07	111.40
0.04	14.01	1.80	171.89	9.09	110.74

0.04	15.35	1.85	175.22	9.10	110.07
0.04	14.68	1.93	182.34	9.41	115.18
0.04	14.68	1.96	181.45	9.76	109.85
0.04	15.79	1.96	179.89	9.81	107.63
0.04	15.12	1.98	181.00	9.83	106.74
0.04	16.01	2.10	189.89	9.85	106.07
0.04	15.35	2.12	187.89	9.85	105.63
0.04	15.12	2.12	186.56	9.86	105.40
0.04	16.01	2.15	187.45	9.88	104.96
0.05	20.24	2.28	196.79	9.88	104.74
0.05	19.79	2.32	195.02	9.89	104.51
0.08	29.13	2.33	193.46	9.89	104.29
0.09	31.35	2.34	192.35	9.89	104.29
0.09	30.91	2.43	199.02	9.89	104.07
0.12	40.47	2.57	203.91	9.90	103.85
0.14	44.47	2.59	200.79	9.90	103.85
0.14	43.81	2.61	199.24	9.90	103.62
0.15	48.03	2.66	202.35	9.90	103.62
0.20	59.60	2.85	209.24	9.91	103.40
0.20	58.48	3.45	136.97	9.91	103.40
0.20	58.48	4.82	133.42	9.91	103.18
0.28	74.04	4.83	132.08	9.91	103.18
0.28	72.27	4.84	131.20	9.91	102.96
0.28	71.60	4.86	130.75	9.92	102.96
0.35	86.06	4.86	130.31	9.92	102.74
0.36	85.61	4.86	130.08	9.93	102.74
0.37	84.28	4.87	129.64	9.93	102.74
0.43	97.39	4.88	129.42	9.93	102.51
0.46	98.50	5.22	136.09	9.93	102.51
0.47	96.95	5.39	132.53	9.93	102.51

THB-6 experimental load vs deflection result in tabular form.

Deflection (mm)	Load (kN)	Deflection (mm)	Load (kN)	Deflection (mm)	Load (kN)	Deflection (mm)	Load (kN)
0.00	0.00	0.57	103.07	1.54	143.32	2.64	80.87
0.00	0.36	0.57	102.89	1.54	143.13	2.65	80.33
0.01	4.16	0.58	102.71	1.54	142.95	2.77	80.14
0.01	5.24	0.58	102.34	1.55	142.77	2.98	78.15
0.01	5.06	0.58	102.34	1.55	142.59	3.04	75.81
0.02	6.68	0.58	101.80	1.55	142.41	3.07	74.54
0.03	10.11	0.59	101.62	1.55	142.23	3.18	75.45
0.03	10.65	0.59	101.62	1.55	142.05	3.30	72.56
0.03	10.47	0.59	101.62	1.55	141.87	3.34	71.30
0.04	14.26	0.62	107.58	1.55	141.69	3.36	70.76
0.05	16.25	0.66	111.73	1.55	141.69	3.37	70.39
0.05	15.70	0.68	112.63	1.56	141.51	3.70	73.10
0.06	19.14	0.69	112.63	1.56	141.51	3.94	70.03
0.07	21.30	0.70	111.55	1.56	141.33	4.02	70.39
0.07	21.12	0.70	111.19	1.56	141.15	4.47	69.67
0.08	23.47	0.71	111.00	1.56	140.97	4.54	67.33
0.09	27.26	0.77	117.69	1.56	141.15	4.88	69.67
0.09	26.36	0.83	121.12	1.59	144.40	5.13	67.87
0.12	31.41	0.87	121.48	1.64	150.17	5.17	66.97
0.12	32.85	0.88	119.85	1.67	152.34	5.19	66.61
0.12	31.77	0.88	119.31	1.69	153.43	5.21	66.24
0.14	38.09	0.91	121.66	1.70	153.43	5.23	65.88
0.14	39.90	0.97	125.63	1.70	152.16	5.23	65.70
0.14	38.81	1.04	129.78	1.70	151.43	5.24	65.70
0.16	42.42	1.06	128.87	1.71	151.25	5.25	65.52
0.18	48.20	1.07	127.97	1.81	159.56	5.26	65.34
0.18	47.11	1.08	127.43	1.85	160.10	5.26	65.34
0.20	50.72	1.09	127.25	1.88	159.74	5.27	65.16
0.23	57.76	1.11	128.33	1.89	158.30	5.27	65.16
0.24	57.58	1.12	128.33	1.89	157.40	5.28	64.98
0.25	56.68	1.13	128.51	1.89	156.85	5.28	64.98
0.29	66.97	1.14	127.97	1.89	156.49	5.28	64.80
0.31	70.03	1.14	127.43	1.90	155.95	5.28	64.80
0.31	68.77	1.14	127.43	1.96	161.00	5.45	68.77
0.31	68.05	1.15	127.25	2.02	165.33	5.70	67.33

0.31	67.69	1.15	127.07	2.05	165.15	5.83	67.87
0.31	67.15	1.17	128.33	2.05	164.07	6.21	65.52
0.31	66.79	1.19	130.32	2.05	163.53	6.29	64.44
0.34	74.37	1.20	130.86	2.05	162.27	6.30	63.90
0.37	79.24	1.20	130.32	2.05	161.91	6.31	63.36
0.38	81.77	1.22	131.04	2.05	161.36	6.32	63.18
0.39	82.67	1.22	130.50	2.06	161.00	6.32	63.00
0.39	82.49	1.22	130.14	2.07	160.64	6.33	63.00
0.39	81.59	1.22	129.96	2.07	160.46	6.35	62.82
0.39	81.05	1.24	131.22	2.08	160.46	6.38	62.82
0.39	80.87	1.24	130.86	2.15	166.42	6.38	62.64
0.39	80.51	1.24	130.50	2.16	166.24	6.39	62.46
0.39	80.14	1.24	130.32	2.20	168.22	6.39	62.46
0.39	86.46	1.24	130.14	2.23	167.68	6.39	62.28
0.39	86.28	1.24	129.96	2.25	167.14	6.39	62.28
0.39	86.10	1.24	129.60	2.28	165.88	6.39	62.28
0.39	85.92	1.25	129.78	2.29	163.53	6.39	62.10
0.39	85.74	1.31	136.10	2.31	161.55	6.39	62.10
0.39	85.56	1.33	137.36	2.33	159.56	6.39	62.10
0.39	85.38	1.35	137.90	2.35	156.85	6.40	61.91
0.40	87.54	1.35	137.54	2.49	143.86	6.40	61.91
0.44	94.58	1.35	136.46	2.53	127.97	6.40	61.91
0.46	97.47	1.36	136.28	2.54	109.92	6.40	61.91
0.46	97.10	1.36	136.10	2.54	101.98	6.40	61.73
0.46	96.56	1.37	136.10	2.55	100.18	6.40	61.73
0.47	96.20	1.39	138.62	2.55	99.10	6.40	61.73
0.47	96.02	1.42	141.33	2.55	98.19	6.40	61.73
0.47	95.66	1.46	144.22	2.55	97.65	6.40	61.73
0.49	97.65	1.48	144.76	2.56	96.92	6.40	61.73
0.49	97.29	1.50	145.48	2.57	98.92	6.40	61.55
0.52	102.89	1.51	146.02	2.57	98.37	6.40	61.55
0.55	105.77	1.53	146.20	2.57	97.29	6.40	61.55
0.56	105.05	1.53	145.12	2.57	95.48	6.40	61.55
0.56	104.51	1.53	144.58	2.57	88.44	6.40	61.55
0.57	104.15	1.53	144.22	2.57	84.84	6.41	61.37
0.57	103.79	1.53	143.86	2.63	83.75	6.41	61.37
0.57	103.43	1.53	143.50	2.63	81.95	6.42	61.37